ERASMUS MUNDUS MASTER IN
MEMBRANE ENGINEERING
FOR A SUSTAINABLE WORLD
EM3E-4SW

With the support of the
Erasmus+ Programme
of the European Union

Surface modification and characterization of membrane for platelet-derived growth factor (PDGF) purification in blood

Thesis submitted to the Faculty of Science at the University of Zaragoza, Spain in partial fulfillment of the requirements for the degree of

Master's degree in Membrane Engineering

Erasmus Mundus Master in Membrane Engineering for a Sustainable World

Abigail ROSALES

July 2020

Related to the Ph.D. program, Membrane for protein separation with designed architecture of biointerface at nanoscale (International ANR, MOSAIC-3D Project)
Laboratoire de Génie Chimique de Toulouse (LGC)
Université Paul Sabatier Toulouse III, France

Adviser:	Patrice BACCHIN	Professor, Université Paul Sabatier Toulouse III, France
Co-advisers:	Charaf MERZOUGUI	PhD, Université Paul Sabatier Toulouse III, France
	Christel CAUSSERAND	Professor, Université Paul Sabatier Toulouse III, France
	Pierre ROBLIN	Dr, LGC, France
	Pierre AIMAR	Dr CNRS, LGC, Université Paul Sabatier Toulouse III, France
Overseer:	Reyes MALLADA	Professor, Universidad de Zaragoza, Spain

www.em3e-4sw.eu
em3e-4sw-project@umontpellier.fr

The Erasmus Mundus Master in Membrane Engineering for a Sustainable Word (EM3E-4SW) is an education program financed by the European Commission - Education, Audiovisual and Culture Executive Agency (EACEA), under Project Number-574441-EPP-1-2016-1-FR-EPPKA1-JMD-MOB. It is also supported by the European Membrane Society (EMS), the European Membrane House (EMH), and a large international network of industrial companies, research centers and universities.

ACKNOWLEDGMENTS

I would like to express my heartfelt gratitude to all my advisers for their guidance and for the knowledge they have shared during my internship. Thank you to all the LGC staff who helped me during the experiments. It has been a privilege to be part of LGC.

Thank you to my friends, classmates, and family for their support, constant encouragement, and for keeping me sane during the pandemic.

Maraming salamat at hanggang sa muli!

RESUMEN

La extracción y purificación del Factor de Crecimiento Derivado de Plaquetas (PDGF) de la sangre podría tener potencial en el cuidado de heridas diabéticas. El procedimiento actual implica múltiples pasos y un proceso de separación más simple podría mejorar su productividad. Este reporte está relacionado con un programa de PhD (proyecto MOSAIC 3D). Uno de los objetivos es modificar la membrana de PVDF con un copolímero que capture plaquetas selectivamente. El copolímero debe evitar interacciones no deseadas con las proteínas sanguíneas o puede conjugarse con ellas e inducir la captura de plaquetas. Este estudio pretende optimizar el procedimiento de recubrimiento utilizando copolímero de bloque de poliestireno con poli (ácido acrílico) e investigar su interacción con las principales proteínas de la sangre: albúmina, ɣ-globulina y fibrinógeno. La concentración, el tiempo de recubrimiento y el proceso operativo fueron variados. La distribución del revestimiento y la adsorción estática de proteínas se estudiaron utilizando mapeo FTIR. 5 mg/mL de concentración de copolímero, 2 horas de recubrimiento, y secado del recubrimiento antes del lavado son las condiciones óptimas de recubrimiento. Las tres proteínas tienen una cantidad similar de adsorción con las membranas prístinas y recubiertas que se atribuye a las cadenas cortas de PAA (sólo 10% en peso del copolímero). La disminución de la permeabilidad al agua de las membranas recubiertas a una concentración de copolímero de 1 y 5 mg/ml es mínima (6,15 y 11,8%, respectivamente). La superficie permaneció recubierta después de la filtración del agua. Se recomienda 1) probar otros copolímeros o usar el copolímero PS-b-PAA con cadenas PAA más largas, 2) investigar la adsorción competitiva de las proteínas, 3) realizar pruebas de filtración con una solución de proteínas para identificar la selectividad de las membranas respecto a cada proteína y evaluar el ensuciamiento.

The EM3E4SW Master is an Education Program supported by the European Commission, the European Membrane Society (EMS), the European Membrane House (EMH), and a large international network of industrial companies, research centers and universities (www.em3e-4sw.eu)

ABSTRACT

The extraction and the purification of platelet-derived growth factor (PDGF) from blood could have a potential in diabetic wound care. The current procedure involves multiple steps and a simpler separation process could improve its productivity. This report is related to a Ph.D. program (MOSAIC 3D project). One of the objectives is to modify PVDF membrane with a copolymer that could selectively capture platelets. The copolymer should avoid unwanted interactions with other blood proteins or it can be conjugated with a blood protein and induce platelet capture. This study intends to optimize the coating procedure using polystyrene-block-poly(acrylic acid) copolymer and investigate its interaction with major blood proteins – albumin, ɣ-globulin, and fibrinogen. Concentration, coating time, and operating process were varied. Coating distribution and static protein adsorption were studied using FTIR mapping. 5mg/mL copolymer concentration, 2h coating time, and drying the coating before washing are the optimum coating conditions. All three proteins have a similar amount of adsorption with the pristine and coated membranes which is attributed to the short PAA chains (only 10wt.% of the copolymer). The pure water permeability decline of the coated membranes at 1 and 5mg/mL copolymer concentration is minimal (6.15 and 11.8% respectively). The surface remained coated after water filtration. It is recommended to 1) test other copolymers or use PS-b-PAA with longer PAA chains, 2) investigate competitive protein adsorption, and 3) conduct filtration tests with protein solution to identify the selectivity of the membrane towards each protein and evaluate fouling.

The EM3E4SW Master is an Education Program supported by the European Commission, the European Membrane Society (EMS), the European Membrane House (EMH), and a large international network of industrial companies, research centers and universities (www.em3e-4sw.eu)

CONTENTS

LIST OF TABLES AND FIGURES

Tables

Figures

The EM3E4SW Master is an Education Program supported by the European Commission, the European Membrane Society (EMS), the European Membrane House (EMH), and a large international network of industrial companies, research centers and universities (www.em3e-4sw.eu)

1. INTRODUCTION

Blood supplies nutrients and oxygen to different parts of the human body which is necessary for survival and development. It is 55% plasma (91% water and 9% proteins, ions, nutrients, wastes, *etc.*) and 45% erythrocytes (red blood cells), leukocytes (white blood cells) and thrombocytes (platelets) (**figure 1.1**). Erythrocytes carry the oxygen, leukocytes are for immune response, and thrombocytes' main function is to stop bleeding through blood clot formation after adhesion to the wall of the damaged vessel. Blood contents can be separated into specific compositions which can resolve health problems.

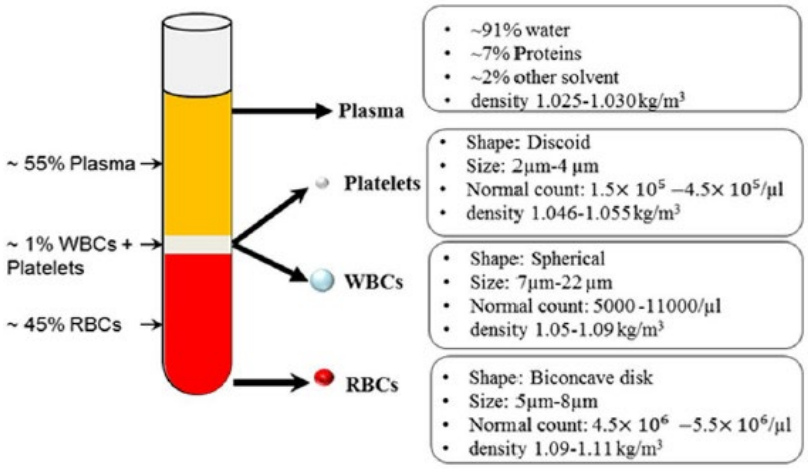

Figure 1.1. Blood components [1]

Membrane process has been a useful technology for blood-related applications such as plasma separation, blood oxygenators, and hemodialyzers where improvement of biocompatibility remains a challenge [2]. Membrane-based plasma separation process separates blood cells (erythrocytes, leukocytes, thrombocytes) from plasma via filtration using hollow fiber membranes with pore sizes between 0.2 to 0.8µm [3]. Blood oxygenators artificially support the life of a patient by supplying oxygen to the blood while removing carbon dioxide [4]. Membranes are of interest due to their similarity to the gas exchange achieved in the lungs. The gas transfer in membrane-type blood oxygenators occurs due to diffusion by exposing the blood to oxygen through a gas-permeable membrane [5]. Hemodialysis is a blood filtration process where toxins and excess water are removed from patients with renal failure

The EM3E4SW Master is an Education Program supported by the European Commission, the European Membrane Society (EMS), the European Membrane House (EMH), and a large international network of industrial companies, research centers and universities (www.em3e-4sw.eu)

diseases [6]. There are two flows on the different sides of the membrane: 1) the bloodstream side containing high toxin concentration and 2) the dialysate side with no or lower toxin concentration. This concentration gradient serves as the driving force of the toxin extraction. Membrane technology has proven to be viable for blood-related applications for decades which still requires further improvement. One way is through the introduction of functional groups on the membrane surface through several surface modification methods. As a result, the modified surface can specifically interact or avoid interaction with the targeted molecules. Thus, particle size difference and affinity become the ruling criteria for the separation process.

1.1 MEMBRANES FOR PLATELET CAPTURE IN BLOOD

Platelet transfusion is necessary for patients undergoing intensive medication (chemotherapy), hematological disease, and surgery [1, 7]. Platelet-derived growth factor (PDGF) is a mitogen that is stored and released by platelets upon activation. It has a significant role in accelerating the wound healing process of diabetic ulcers. The global occurrence of diabetes among people over 18 years of age has increased from 4.7% in 1980 to 8.5% in 2014 [8] implying an increasing demand for diabetes-related treatments.

The current PDGF extraction and purification methods are centrifugation [2] and chromatography [9]. Centrifugation is fast but energy demanding. Chromatography is effective on separation [10], however, it requires a discontinuous operation and has low yield limiting its use on a large-scale production. This necessitates the development of an alternative process for a faster and efficient recovery of diabetic-related wounds. Separation by porous membrane is an alternative since the membranes can be functionalized through surface modification allowing it to specifically interact with the targeted components resulting in selective separation. The idea is to design a membrane system that can 1) capture the platelets from the blood, 2) enable activation of the platelets and release of PDGF, and 3) release the captured platelets to give way for the fresh platelets. In this way, it avoids the discontinuous process, reduces the equipment requirements, and simplifies the process for PDGF purification. Consequently, it can reduce the treatment cost. Currently, there is no membrane system with this design.

Synthetic hydrophobic polymeric membranes, such as polyvinylidene fluoride (PVDF) among others, are usually chosen for blood separation research [11] due to its sufficient thermal, mechanical, and chemical resistance preventing damages during the manufacture and sterilization steps [2]. Also, its manufacturing process is cost- and time-effective. However, blood cells and proteins are usually partially hydrophobic. Thus, hydrophobic polymers are not bioinert and selective such that they interact with blood cells and proteins resulting in unwanted phenomena such as biofouling. Hence, membrane surface modification with functional groups could be a solution that we propose.

The membrane interface with the blood should comprise of these combinations: 1) bioinert or non-fouling functional groups to have minimum adhesion of unwanted blood components, 2) functional groups promoting selective interaction with the platelets, and 3) a brush that is stimulus responsive to promote attachment and detachment of cells (**figure 1.2**).

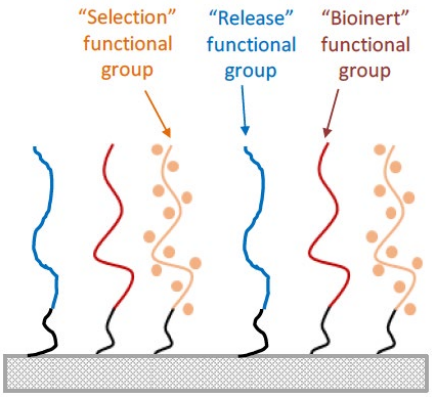

Figure 1.2. Schematic representation of the membrane design [12]

How do we promote selective interaction with platelets? One way is to find a material that has preferential interaction with platelets and not with other blood proteins. The other possible solution seems to lie in human bodies. Since the 1970s, it has been known that blood protein adsorption on hydrophobic polymers triggers platelet adhesion [13] which is still an issue nowadays in polymeric membranes' hemocompatibility. Globulin, albumin, and fibrinogen are the major blood proteins. In an event of injury, blood clot formation takes place by platelet adhesion to the site of injury and to each other (aggregation) forming a plug to avoid blood loss. Fibrinogen's role in blood clot formation is to promote platelet aggregation [14] which can be analogous to a glue holding the platelets together. Mimicking this physiological process

to selectively capture platelets is worth investigating. A study showed that under experimental conditions, even inactivated platelets resulted in adhesion to purified fibrinogen substrate [15]. Also, adsorption of globulin and most notably, fibrinogen, on a foreign surface was found to enhance platelet adhesion while albumin has the opposite effect [13]. Another study has shown that: fibrinogen-coated substrate resulted in platelet adhesion to the surface with little release of platelets; gamma globulin-coated substrate lead to platelet adhesion, aggregation, and release of platelet constituents; and albumin-coated surface caused little adhesion from platelets [16]. Thus, platelet capture using a membrane, surface-modified with blood protein such as fibrinogen or globulin, could also be a possible solution.

1.2 SURFACE MODIFICATION

Grafting and coating are common surface modification processes at it allows control of grafting or coating density, thickness of the modifying layer, and chemistry (through polymer material choice) without significantly changing the structure of the membrane. Grafting processes establish covalent bonding between the surface modifier and the membrane surface through grafting from or onto techniques. It creates stronger interactions resulting in better stability than coating processes. In grafting from, polymer grows from the membrane surface by putting the membrane in contact with a monomer solution given that there is additional energy supplied to initiate the polymerization and to activate the membrane. While in grafting onto, a known composition of polymer covalently bonds to the surface activated membrane. Both grafting methods require additional energy and time-consuming multiple step process which generate high costs. Also, membrane pretreatment with alkali solution or irradiation can damage the properties and structure of the membrane, thereby affecting the membrane's performance.

Conversely, coating is readily achieved through immersion, spray coating, dip-coating, and spin coating making it suitable for large-scale production at a reduced cost. In this process, surface-modifying molecules self-assemble on the surface of membrane establishing non-covalent interactions. For example, it could be a functional copolymer with hydrophobic groups forming a strong affinity with a hydrophobic membrane. Since surface modifiers

interact with the membrane through non-covalent interactions, it may not be stable resulting in detachment from the membrane surface. Thus, the success of the coating depends on the extent of interaction between the surface modifier and the membrane surface.

1.3 POLYMERS USED IN SURFACE MODIFICATION

Hydrophilic polymer polyethylene glycol (PEG) and its derivatives are one of the most studied polymers to prevent adsorption of blood proteins, blood cells, and bacteria. PEGylated copolymers on membranes enhance the trapping of water at its surface through hydrogen bonding leading to the formation of hydration layer which gives a physical and energetic barrier against protein, cells, and bacteria [17]. Consequently, biofouling on the membrane is reduced. To ensure the stability of these polymers on the membrane's surface, they are usually combined with a hydrophobic block that will interact with the hydrophobic membrane surface. Chiag *et al.* used polystyrene (PS) block to anchor the hydrophilic poly(ethylene glycol) methacrylate (PEGMA) block to the hydrophobic PVDF surface which made the membrane resistant to bovine serum albumin (BSA), *Escherichia coli* and *Stenotrophomonas maltophilia* [18]. Other studies have also shown that PVDF membrane modified with PS/PEGMA block copolymer reduces the adhesion of platelets, erythrocytes, leukocytes, and fibrinogen [19, 20]. Tuning the amount of the polymer blocks coated on the membrane's surface allows control of the hydrophobic/hydrophilic balance resulting in tunable fouling resistance.

Poly(N-isopropylacrylamide) (PNIPAAM) is a temperature-responsive polymer that undergoes a rapid transition from a hydrophilic to a hydrophobic structure in water at its lower critical solution temperature (LCST) between 30 and 35°C [21]. It swells (hydrophilic) at temperatures below its LCST due to hydrogen bonding between the water and PNIPAAM molecules, and it collapses (hydrophobic) at temperatures above its LCST due to preferred intramolecular interaction among PNIPAAM molecules (**figure 1.3**). This means that its hydrophilicity and consequently, cell, protein, and bacterial adhesion behavior can be regulated with temperature which can be further controlled through the incorporation of other anti-fouling functional groups as demonstrated by several studies [22-24]. Thus, PNIPAAM can be

considered as the stimulus-responsive functional group in the proposed membrane design due to its thermoresponsive and tunable bioadhesive properties.

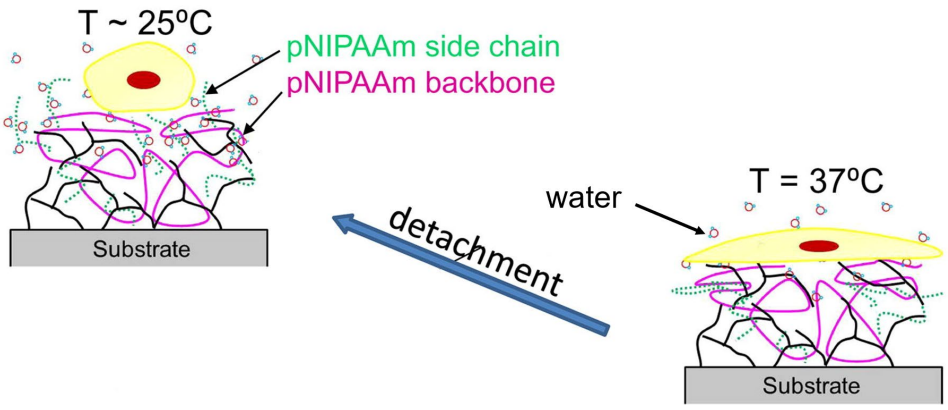

Figure 1.3. Schematic representation of cell detachment at T<LCST (left) and cell attachment at T>LCST (right) [25]

Yu et al. demonstrated that human serum albumin (HSA), a blood protein, has strong attractive interaction with poly(acrylic acid) (PAA) on certain conditions where both are negatively charged [26]. Also, other researchers demonstrated that albumin polymer could be conjugated with fibrinogen and it successfully attached to a platelet-immobilized surface [27]. Thus, it would be interesting to investigate the interactions of blood proteins (HSA, fibrinogen, and globulin) with PAA and verify the potential use of protein-modified PAA to selectively interact with platelets.

Stem cell culture, like PDGF purification, is typically done in batch. However, Peng *et al.* [28] proposed continuous harvesting of stem cells using modified PS-b-PAA brushes for selective interaction with cells of interest, PEGMA hydrophilic brushes to improve fouling resistance and accelerate cell detachment, and PNIPAAM thermoresponsive brushes for controlling the attachment/detachment of cells. This method simplifies the process for stem cell culture and can reduce the costs of therapies which can be potentially applied to PDGF purification.

1.4 CHARACTERIZATION USING FOURIER-TRANSFORM INFRARED SPECTROSCOPY (FTIR)

FTIR will be used in this study due to its ease of operation and simplicity. In FTIR, the absorption intensity relies on the molecule's change in dipole moment as a result of the absorption. Consequently, functional groups containing polar bonds, such as O-H, C=O, and NH, are detected easily with FTIR, while detection of nonpolar groups can be difficult [29]. However, membrane samples should be analyzed in its dry state since OH group absorbs strongly in the infrared region and could obscure other interesting bands.

FTIR can be combined with attenuated total reflectance (ATR) technique which is useful for surface characterization rather than the bulk. In this mode, the sample is placed in contact with a crystal made from high refractive index transparent material. The incident infrared light is focused on one end of the crystal at a certain angle and it undergoes several total internal reflections in the crystal until it reaches the detector (**figure 1.4**). The incident beam penetrates slightly onto the sample at each reflection, which results in a spectrum describing the surface chemical composition of the sample. However, the use of rough and highly porous membranes decreases the contact between the membrane and the crystal which could disturb the measurements [29].

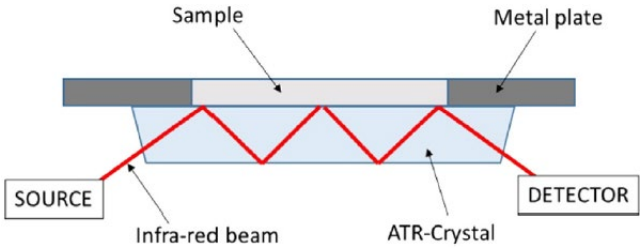

Figure 1.4. Schematic representation of FTIR-ATR operation [30]

An extension of the FTIR technique, FTIR microspectrometry, can qualitatively identify the coating layer and foulants and their distribution over the membrane's surface at millimeter or centimeter scale. In this method, FTIR is equipped with a microscope and specialized detectors which allow scanning of a surface and generation of its chemical map.

FTIR mapping was used to study the fouling behavior of different backwash water sources on ultrafiltration membranes for shale gas desalination [31]. Some researchers used FTIR-ATR

mapping to investigate the composition and distribution of the fouling layer formed on polypropylene (PP) and polytetrafluoroethylene (PTFE) membranes during ammonia stripping via membrane distillation and after using different cleaning techniques [32]. Also, FTIR maps were used to study the heterogeneity of PS-PEGMA copolymer coating on PVDF membrane using various coating concentration and coating time and to investigate the fouling behavior of BSA on surface-modified PVDF membranes [33]. In this study, results showed that FTIR mapping is a more sensitive technique than coating density. The researchers developed a method that assessed the heterogeneity of the coating and adsorbed foulant by defining different coating and adsorption levels. Also, FTIR enables detection of coating and adsorbed proteins at the same time in the same area while other methods require separate preparation of the samples to analyze coating and foulant present on the surface. Hence, FTIR can be a promising technique that we can use for the study of membrane's surface modification and anti-fouling properties.

1.5 OBJECTIVES OF THE STUDY

This report is related to a Ph.D. program (MOSAIC 3D project). One of the objectives is to modify PVDF membrane with a copolymer that could selectively capture platelets while letting other blood components to pass through. The copolymer should avoid unwanted interactions with other blood proteins, or it can be conjugated with a blood protein and induce platelet capture. This study intends to optimize the coating procedure using polystyrene-block-poly(acrylic acid) (PS-b-PAA) copolymer as the surface modifier and investigate its interaction with major human blood proteins – albumin, ɣ-globulin, and fibrinogen. This report aims to:

1) propose an optimum coating conditions of PVDF membrane with PS-b-PAA
2) determine the effect of coating on the membrane's permeability during water filtration
3) investigate the static adhesion of human blood proteins on the copolymer

Results obtained can contribute to the knowledge and development of diabetes-related wound care.

2. MATERIALS AND METHODS

2.1 MATERIALS

Commercial polyvinylidene fluoride (PVDF) microporous membranes (VVHP, Millipore Co.) with an average pore size of 0.1µm and thickness of 125µm were used as-received for the experiments. The polystyrene-block-poly(acrylic acid) ($(PS)_{275}$-b-$(PAA)_{30}$) copolymer, was bought from Sigma-Aldrich. Absolute ethanol ($EtOH_{abs}$) and tetrahydrofuran (THF) used to solubilize the copolymer were purchased from VWR Chemicals Avantor® and Acros Organics, respectively. Phosphate buffered saline (PBS) solution 10x (BP399, Fisher BioReagents) was diluted to PBS 1x using ultrapure water (pH=7.4). Ultrapure water was purified using ELGA PURELAB Prima purification system with an ELGA PURELAB Classic water purification system (final minimum resistivity of 18 MΩcm). 0.5cm^2 membrane area was used for all analyses except for the permeability measurements. Fibrinogen from human plasma (F3879), ɣ-globulins from human blood (G4386), and albumin from human serum (A1653) were bought from Sigma-Aldrich.

Table 2.1. $(PS)_{275}$-b-$(PAA)_{30}$ properties [34]

Formula	M_n (Da) 1Da=1g/mol	Polydispersity index (PI)	Degree of polymerization (DP)
$(PS)_{275}$-b-$(PAA)_{30}$	PAA: 1000-2000 PS: 27000-31000	≤1.1	PAA: 30 PS: 275

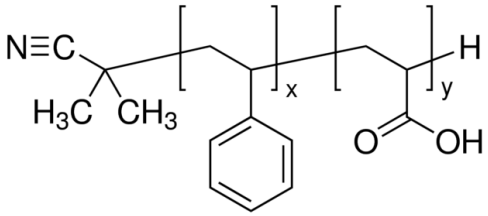

Figure 2.1. Molecular structure of $(PS)_{275}$-b-$(PAA)_{30}$ where x=repeating units of PS polymer and y=repeating units of PAA polymer [34]

2.2 METHODS

2.2.1 COATING OF THE MEMBRANES

Operating process, coating time, and copolymer concentration were varied to optimize the coating procedure using 50% (v/v) $EtOH_{abs}$-THF solvent. The copolymer solutions were prepared by dissolving and mixing the desired weight of $(PS)_{275}$-b-$(PAA)_{30}$ in the solvent.

PVDF membranes were immersed in Eppendorf tubes® containing 1mL of copolymer solution at desired concentration and time. One PVDF membrane was immersed in the solvent as a control. Drying time was 2h at 40°C while washing was done twice using $EtOH_{abs}$ to remove the non-adsorbed copolymer. In the optimization, these conditions were followed with only one variable changing.

Two operating processes were tested with the following order of procedure: 1) Immersion - Washing - Drying (IWD) and 2) Immersion - Drying - Washing (IDW). For the rest of the optimization tests, IDW was used. To optimize the coating time, PVDF membranes were immersed for 1h, 2h, and 4h using 5mg/mL copolymer concentration. Copolymer concentration was also varied from 0.5 to 10mg/mL using 2h coating time.

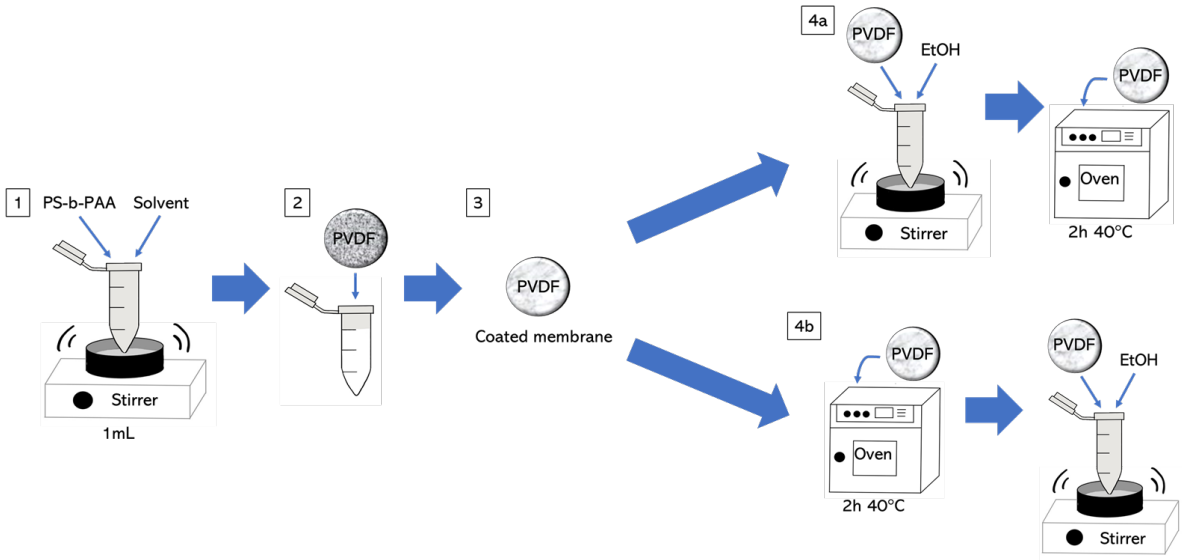

Figure 2.2. Illustration of the coating procedure of PVDF membranes with the following steps: 1) copolymer solution preparation, 2) membrane immersion, 3) coated membrane, 4a) IWD, 4b) IDW. In optimization, step 1 was varied from 0.5 to 10mg/mL copolymer concentration, and step 2 was varied at 1h, 2h, and 4h coating time.

2.2.2 STATIC PROTEIN ADSORPTION

Each protein was prepared by dissolving 1mg of the desired protein in 1mL of PBS 1x. They were prepared the day before the adsorption experiment and kept refrigerated. The membrane was modified according to the optimum conditions. It was immersed in 1 mL of PBS 1x overnight to hydrate the copolymer structure. Afterwards, PBS 1x was replaced by 1mg/mL of protein solution for 2h at room temperature. Then, it was washed with PBS three times to remove the non-adsorbed proteins followed by drying in the oven for 2h at 35°C. Three sets (one for each protein) with four samples were used for each static protein adsorption test: 1) pristine membrane immersed in protein, 2) pristine membrane immersed just in PBS, 3) coated membrane immersed in protein, and 4) coated membrane immersed just in PBS.

2.2.3 CHARACTERIZATION

Attenuated total reflectance Fourier transform infrared spectroscopy (ATR-FTIR, Nicolet 6700, Thermo Scientific) with diamond crystal, 45° incident angle, 16 scans, and 4 cm^{-1} spectral resolution was used to obtain spectra and verify the presence of the coating and the proteins. Air was used as background and all spectra were recorded over the wavenumber range from 4000 to 400 cm^{-1}. The obtained spectra were unprocessed except for baseline alignment to qualitatively compare absorbance peak heights. Raw spectra are available in **Section A.2 of the Appendix**. Beer-Lambert Law (**equation 2.1**) states that absorbance is proportional to concentration. Thus, when comparing similar material, a higher absorbance peak means higher concentration on the surface.

$$A = \varepsilon c l \qquad \textbf{(equation 2.1)}$$

where ε is absorptivity ($M^{-1}cm^{-1}$), c is concentration (M), and l is optical path length (cm).

ATR-FTIR (iN10 infrared microscope, Thermo Scientific) with germanium crystal, 25° incident angle, $8cm^{-1}$ spectral resolution, and 16 scans for each point was used for surface chemical mapping to determine the coverage of the coating and the protein adsorption. 60x60 points were measured and each point has 50x50um area. Dried samples were taped onto the microscope glass slides then analyzed. To generate the chemical maps, first, peaks of interests that confirm the presence of the coating and proteins were identified. Peaks with the highest absorbance and unique to the material of interest are chosen for the chemical mapping. Then,

the peak height was measured by taking the baseline limit. The chemical maps generated are color-coded according to absorption peak height intensity from blue (lowest intensity) to red (highest intensity). A higher peak intensity indicates more coating or protein is present on the surface. All maps generated are unprocessed.

2.2.4 PERMEABILITY MEASUREMENT

Preparation for permeability measurement

Before the filtration tests, precautions should be considered to obtain accurate data. First, the hydrophobicity of the membrane could result in lower transport characteristics. To overcome this in the experiments, 5mL of ethanol was first filtered through the membrane to help wet the membrane. Second is membrane compaction. It is the compression of the membrane due to applied pressure resulting in the unsteady and declining transport properties [35]. It cannot be avoided; however, a steady-state performance is achieved if the membrane is compacted before the measurements. To compress the membrane, dead-end filtration was conducted on the membrane using Amicon® cell (Series 8010, Merck Millipore) and ultrapure water. The pressure was set to 0.15MPa (1.5bar) for a few hours until the flux stabilized.

Permeability measurement of pristine and modified membranes

The permeability of the pristine membrane was measured by using the compacted membrane and the previous set-up where pressure was varied from 0 to 0.1MPa (0 to 1bar). For each pressure, the weight of the permeate was obtained every 5 minutes for four times to observe the instantaneous flux change and verify its stability. To check if the coating has a significant impact on the membrane's permeability, compacted membranes were coated using 1 and 5mg/mL copolymer concentration at optimum conditions. Afterwards, similar steps for pressure variation and weight measurement were followed. Flux, J (kg/m^2s), was calculated using a filtration area of $3.80cm^2$. Flux vs pressure was plotted. Using Darcy's Law (**equation 2.2**), and the slope of the plot, permeability was obtained.

$$J = \frac{\Pi \, \Delta P}{L} \qquad \textbf{(equation 2.2)}$$

where Π is permeability ($kg.m/m^2.s.MPa$), P is pressure (MPa), and L is membrane thickness of 125μm.

3. RESULTS AND DISCUSSION

The results of the 1) coating procedure optimization of PVDF membrane with PS-b-PAA, 2) impact of coating on the membrane's permeability during water filtration, and 3) static adhesion of human blood proteins on the copolymer will be discussed to evaluate its potential for platelet capture. Before proceeding with the analysis, FTIR spectra of the PVDF pristine membrane and powder $(PS)_{275}$-b-$(PAA)_{30}$ were compared (**figure 3.1**). Based on the molecular structure of the copolymer (**figure 2.1**), the PS and the polymer backbone can be seen on its spectrum with their peaks summarized in **table 3.1**. Also, the obtained $(PS)_{275}$-b-$(PAA)_{30}$ spectrum is similar to the spectrum of PS in literature [36] (**figure 3.2**).

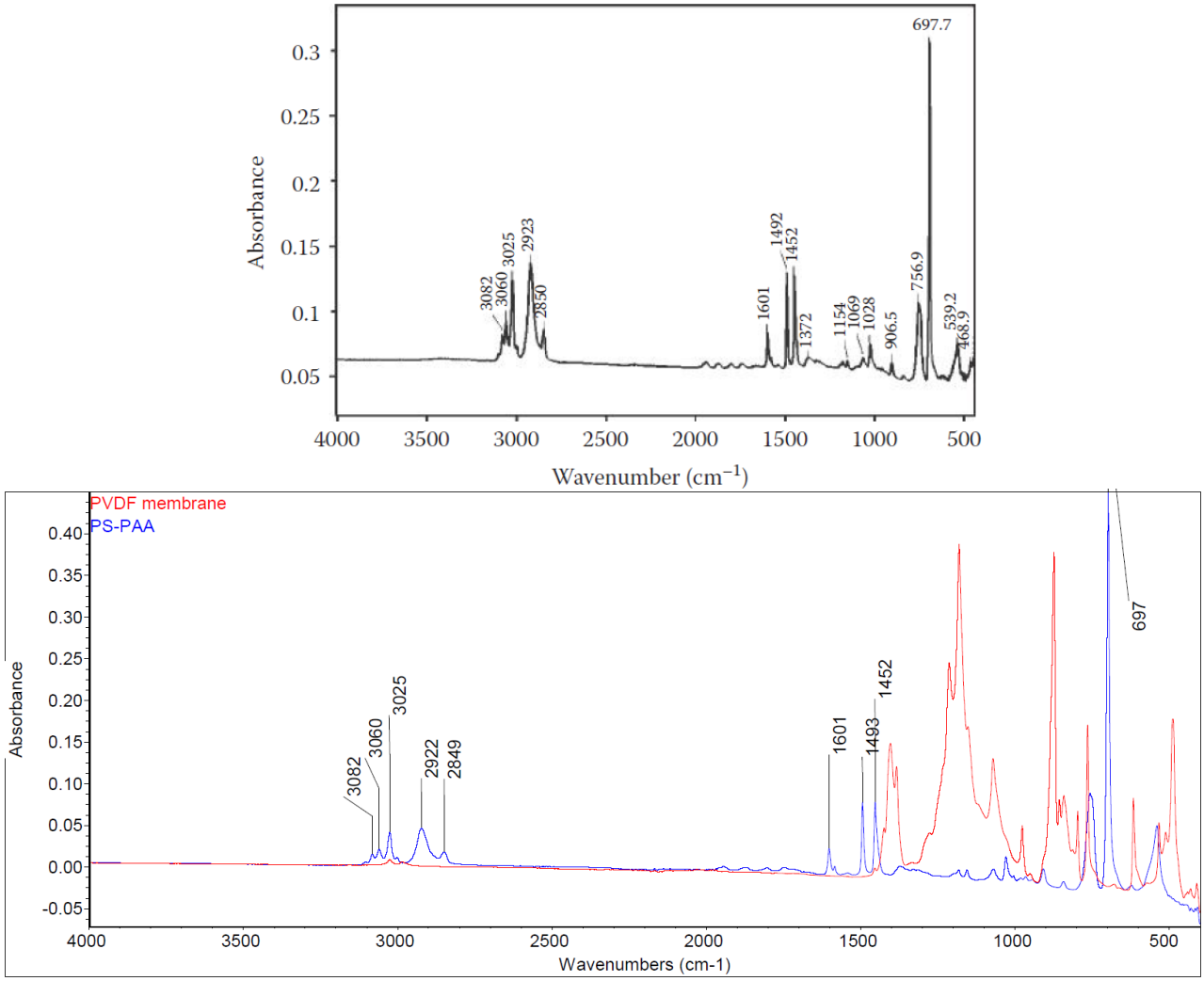

Figure 3.1. (top) IR spectrum of PS [36] and (bottom) spectra of $(PS)_{275}$-b-$(PAA)_{30}$ and PVDF pristine membrane

Table 3.1. Absorption of functional groups in $(PS)_{275}$-b-$(PAA)_{30}$

Absorption (cm^{-1})	Functional groups [37]
3105-3000	=C-H stretching in PS
3000-2850	-C-H stretching in the polymer backbone
1600, 1500, 1450	C=C stretching of the aromatic in PS
700	C-H deformation of monosubstituted aromatic in PS

Ideally, the spectrum of carboxylic acid in PAA should have absorption at 1) 3300-2500 cm^{-1} attributing to O-H stretching, 2) ~1700cm^{-1} for C=O stretching, and 3) 1440-1395 due to O-H deformation [37, 38]. However, none of these were observed. This can be due to the small length of PAA in comparison with PS (copolymer is 10 wt.% PAA). Absorption peak at 700 cm^{-1} was chosen for all the spectra and mapping presentation of the coating due to its strong absorbance and non-overlap with the peaks of the membrane. For the complete FTIR spectra of the samples, refer to **Section A.2 of the Appendix**.

3.1 OPTIMIZATION OF THE COATING PROCEDURE

In this study, PS polymer is the anchoring block to the PVDF as a result of their hydrophobic interactions, while PAA polymer forms a hydrophilic layer. Operating processes, copolymer concentrations, and coating times were varied to identify the procedure that will result in stable and good coating coverage using 50 % (v/v) $EtOH_{abs}$-THF as the solvent. For the study on the choice of solvent, refer to **Section A.2.1.1 of the Appendix**.

3.1.1 VARIATION OF OPERATING PROCESS

Two operating processes were tested with the following order of procedure: 1) Immersion - Washing - Drying (IWD), 2) Immersion - Drying - Washing (IDW). FTIR maps and spectra at 700cm^{-1} show that copolymers adhered to the membrane's surface and there is more copolymer presence with IDW than IWD (**figures 3.2 and 3.3**). This suggests that washing

after drying results in better copolymer adhesion than washing immediately after immersion. The latter means that the solvent ($EtOH_{abs}$/THF) and ethanol used for washing are both present in the environment which could mean that the interaction between the copolymer and the surrounding medium is slightly stronger than the hydrophobic interaction between the copolymer and the membrane resulting in partial removal of the coating. Meanwhile, if washing was done after drying, the solvent has already dried out in between the brushes before washing. This could ensure stronger hydrophobic interactions leading to better copolymer adhesion. Thus, the chosen operating process for this study is IDW.

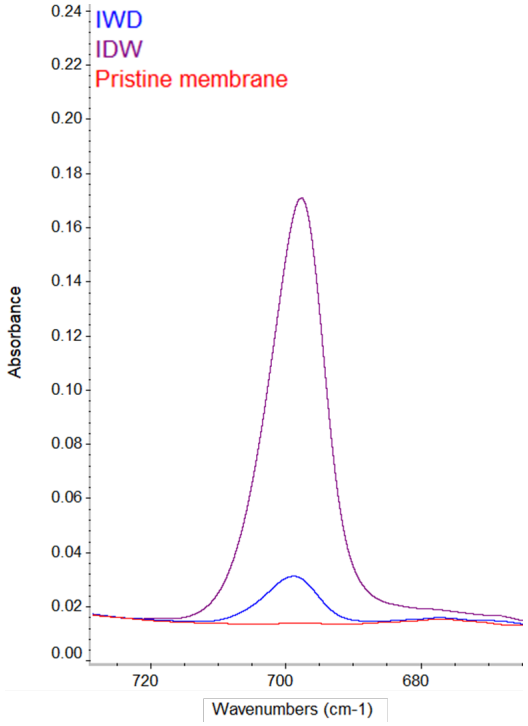

Figure 3.2. FTIR spectra at 700cm^{-1} of coated membranes at different operating processes: 1) Immerse - Dry - Wash - Dry (IDW) and 2) Immerse - Wash - Dry (IWD)

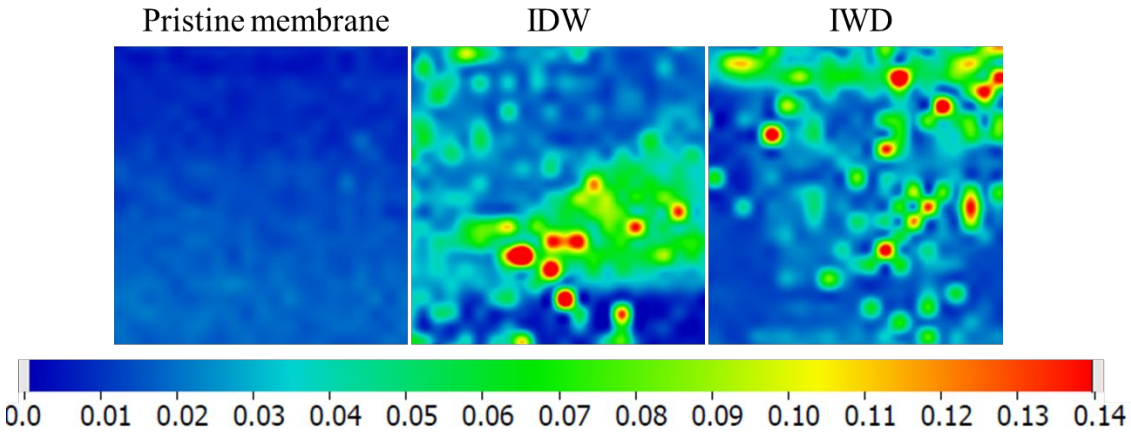

Figure 3.3. FTIR maps at 700cm^{-1} of coated membranes at different operating processes

3.1.2 VARIATION OF COATING TIME

The presence of the copolymer coating on the membrane's surface is evident for 1h, 2h, and 4h coating time. One would expect an increase in coating amount with coating time since the copolymers are given enough time to self-assemble on the surface until a plateau is reached indicating saturation of the surface. However, the results show an increase of coating at 2h followed by a decrease at 4h (**figures 3.4 and 3.5**). Thus, 2h was the chosen optimum coating time.

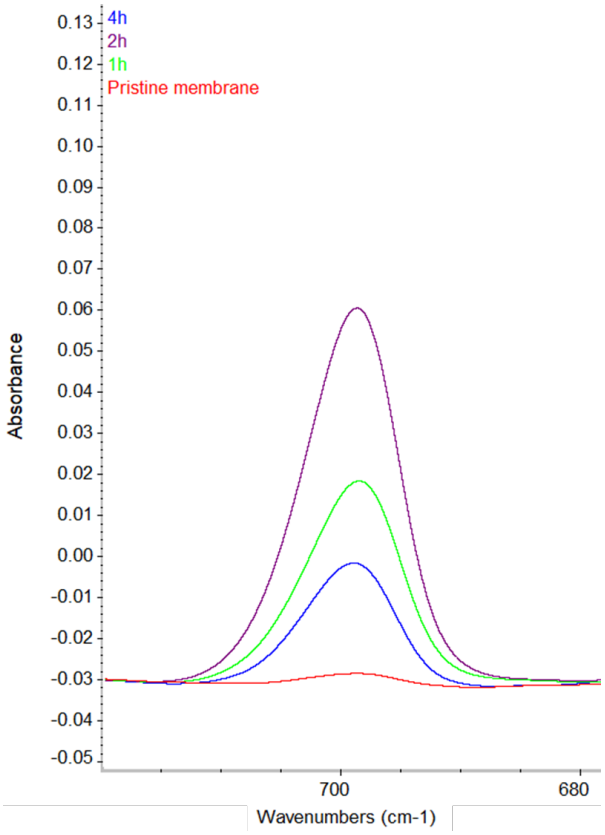

Figure 3.4. FTIR spectra at 700cm^{-1} of membranes at varying coating time (1h, 2h, and 4h)

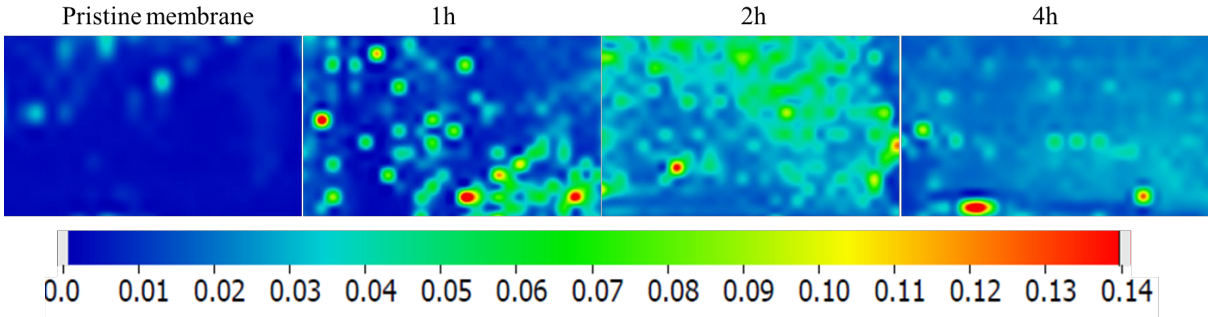

Figure 3.5. FTIR maps at 700cm^{-1} of membranes at varying coating time (1h, 2h, and 4h). The map was truncated in this case to remove some artifacts.

3.1.3 VARIATION OF COPOLYMER CONCENTRATION

The concentrations from 0.5 to 10mg/mL were first investigated. FTIR spectra show an increase in coating with copolymer concentration (**figure 3.6**). Since 0.5mg/mL and 10mg/mL have small and high absorbance respectively, intermediate concentrations at 1, 3, and 5mg/mL were chosen for FTIR mapping to confirm the coating coverage. FTIR maps (**figure 3.7**) show that 5mg/mL sufficiently covers the membrane implying that using 10mg/mL would be excessive. Thus, 5mg/mL was chosen as the optimum copolymer concentration.

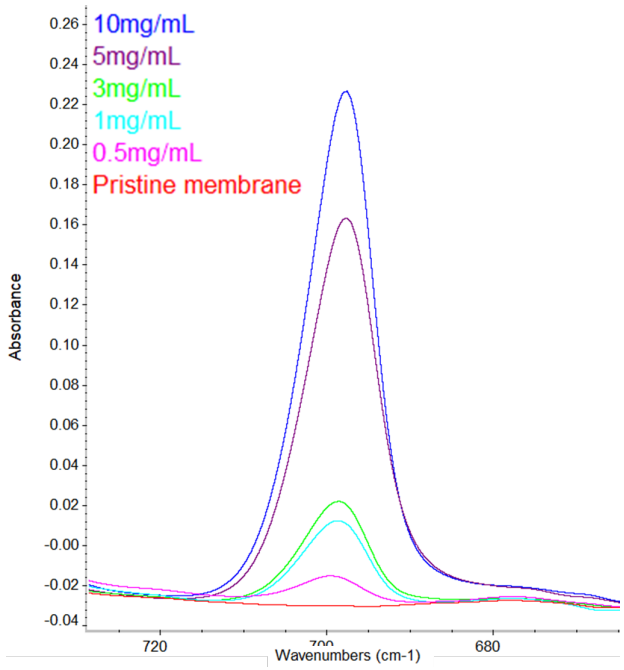

Figure 3.6. FTIR spectra at 700cm^{-1} of coated membranes at varying copolymer concentration (0.5 to 10mg/mL)

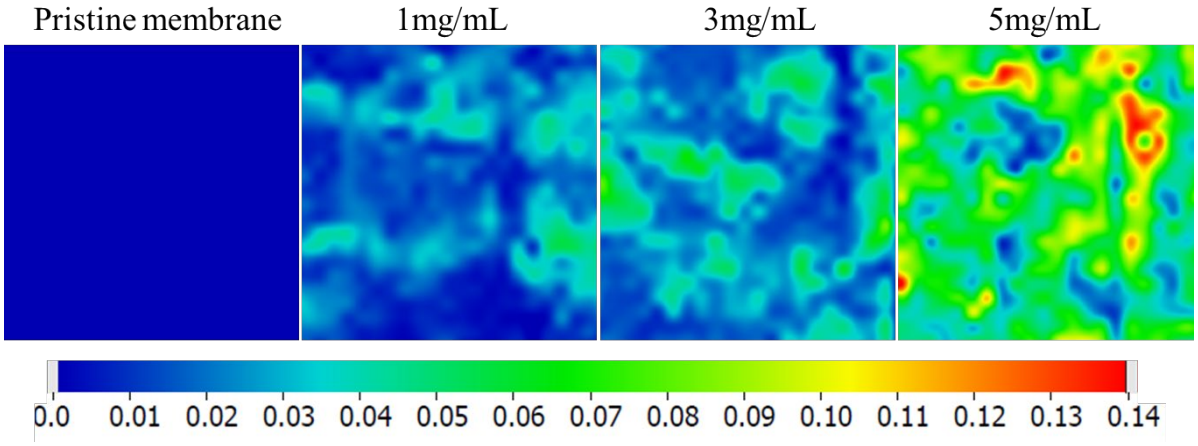

Figure 3.7. FTIR maps at 700cm^{-1} of coated membranes at varying copolymer concentration (1, 3, and 5mg/mL)

3.2 PERMEABILITY MEASUREMENT

Pure water permeability of pristine and coated membranes (using 1 and 5mg/mL copolymer concentration) was investigated. The permeability is equal to the slope of the curve (**figure 3.8**) multiplied by the membrane's thickness as per Darcy's Law.

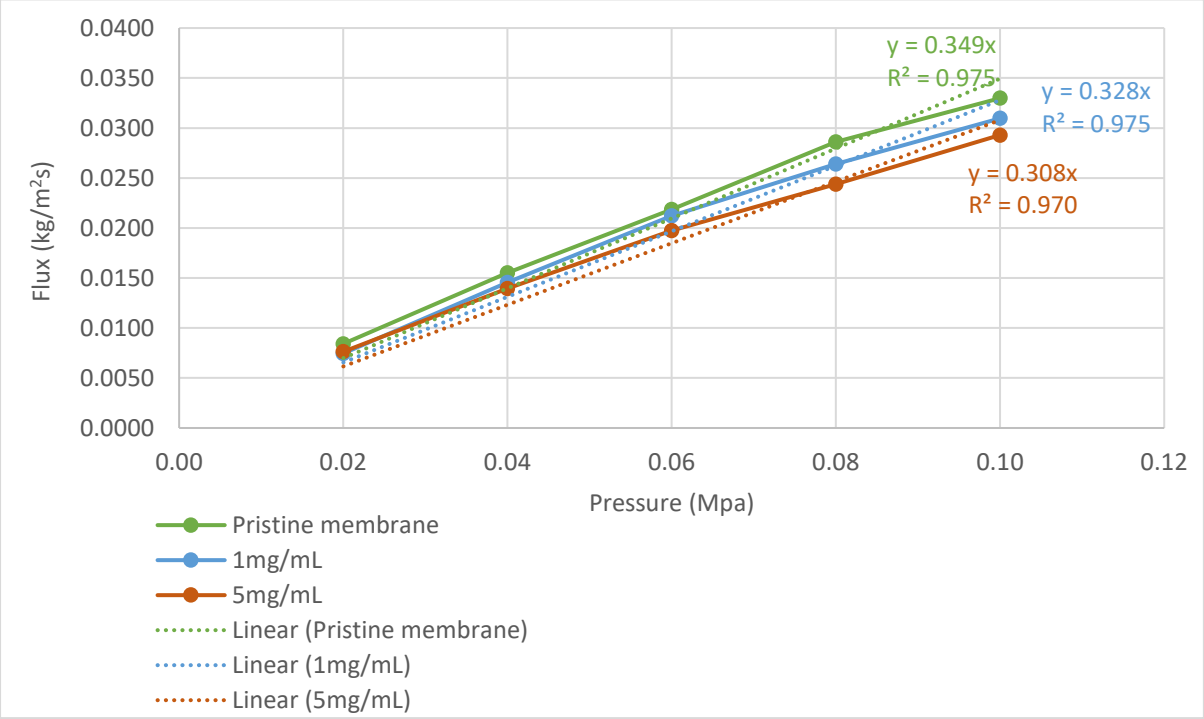

Figure 3.8. Flux evolution of pristine and coated membranes (1 and 5mg/mL copolymer concentration) with pressure

Table 3.2. Calculated pure water permeability and the percent decline after coating

	Permeability 10^{-5} (kg.m/m^2.s.MPa)	Permeability % decline after coating
Pristine membrane	4.37	-
Membrane coated at 1mg/mL	4.10	6.15
Membrane coated at 5mg/mL	3.85	11.8

The fluid viscosity and resistance are supposedly constant in this experiment, thus, flux is expected to increase proportionally with pressure. However, the measured fluxes deviate from the straight line suggesting that it does not completely follow Darcy's Law. Considering that

the fluxes were measured by increasing the pressure, it could due to the unswelling of the membranes upon increase of pressure resulting in the deviation from the straight line. The slope decrease at increasing pressure could also be due to incomplete compaction of the membrane which can be seen as a slight decrease of flux through time at a constant pressure of 0.15MPa (1.5bar) (**figure 3.9**). Thus, it is recommended to further confirm these by measuring the permeability from higher pressure to lower pressure and observe if there would be a hysteresis.

After coating, the permeabilities decreased for both copolymer concentrations (**table 3.2**) as a result of the additional resistance to the system by the coating. However, the percent decline for both concentrations is minimal.

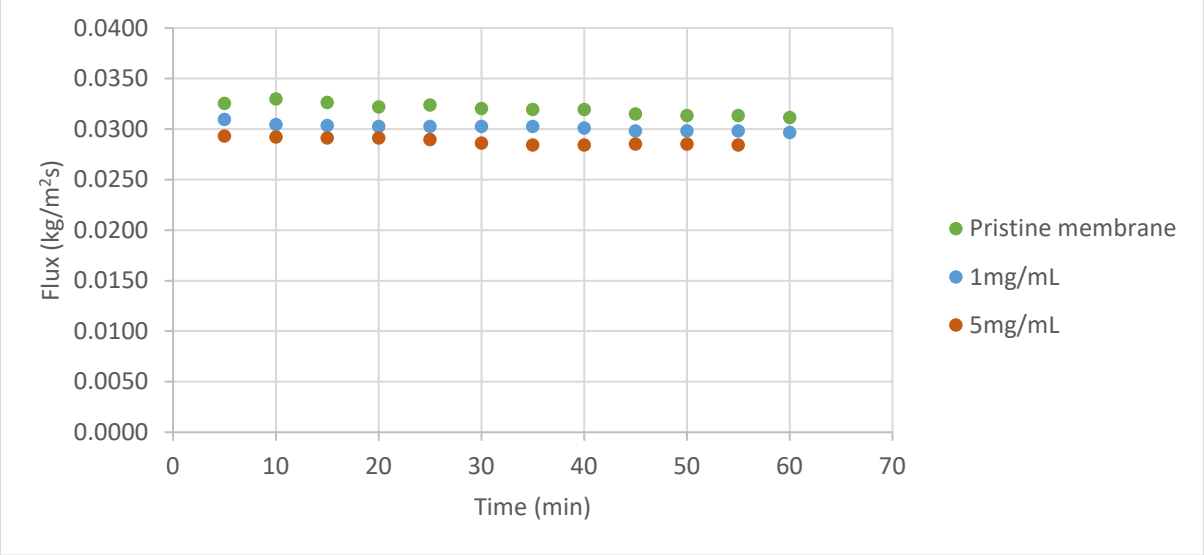

Figure 3.9. Flux through time of pristine and coated membranes (1 and 5mg/mL copolymer concentration) at 0.15MPa (1.5bar)

FTIR spectra of the coated membranes after pure water filtration were collected to verify the stability of the coating. Results show that the coating is still present for both concentrations indicating that the coating remained on the surface even after water filtration (**figure 3.10**). At 1mg/mL coating, there were peaks at 3700-3000cm^{-1} and 1750-1600cm^{-1} which could be due to water [37]. At 5mg/mL, only the copolymer peaks are visible (no water and PVDF membrane peaks) implying that there was a relatively thick layer of copolymer on the surface.

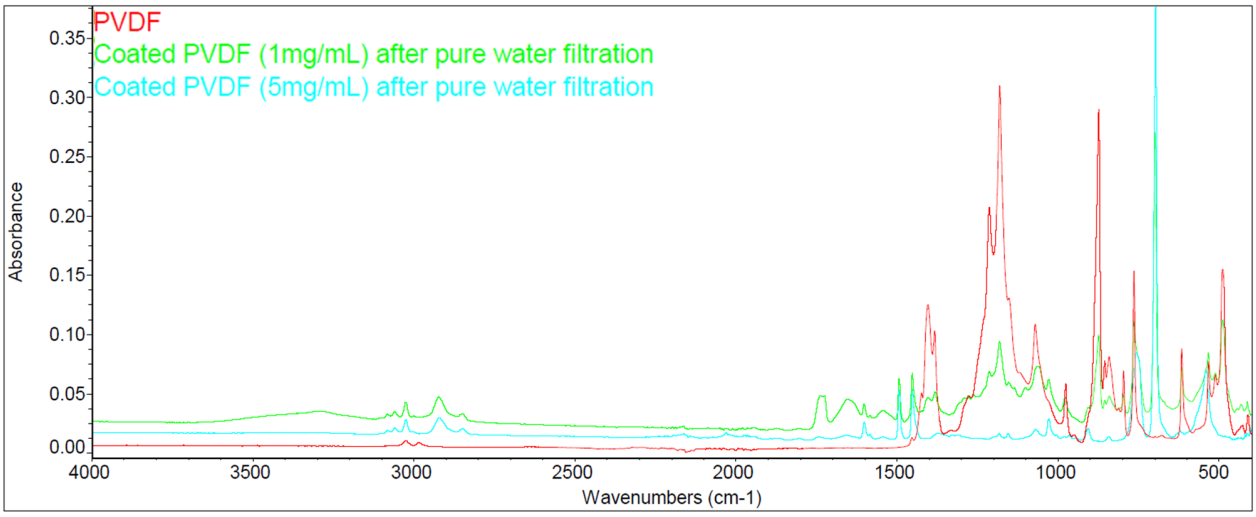

Figure 3.10. FTIR spectra of pristine and coated membranes (1 and 5mg/mL copolymer concentration) after pure water filtration

3.3 STATIC PROTEIN ADSORPTION

Adsorption of albumin (HSA), globulin, and fibrinogen with the pristine and coated membranes was studied. Pure spectra of the proteins in their powder form were obtained (**figure 3.11**). Proteins are made of different amino acids connected by peptide bonds (amide). Their general structure is complicated. However, it is known that all amino acids have N-H and C=O groups suggesting that these could be the most abundant functional groups in proteins. Therefore, notable peaks observed in the FTIR spectra could be due to these groups (highlighted in blue in **figure 3.11,** summarized in **table 3.3**).

Table 3.3. Absorption of functional groups in proteins

Absorption range (cm^{-1})	Functional groups [37]
3500-3070	Amide N-H stretching vibration
1680-1630	Amide C=O stretching vibration
1570-1515	Amide N-H deformation and C-N stretching vibrations

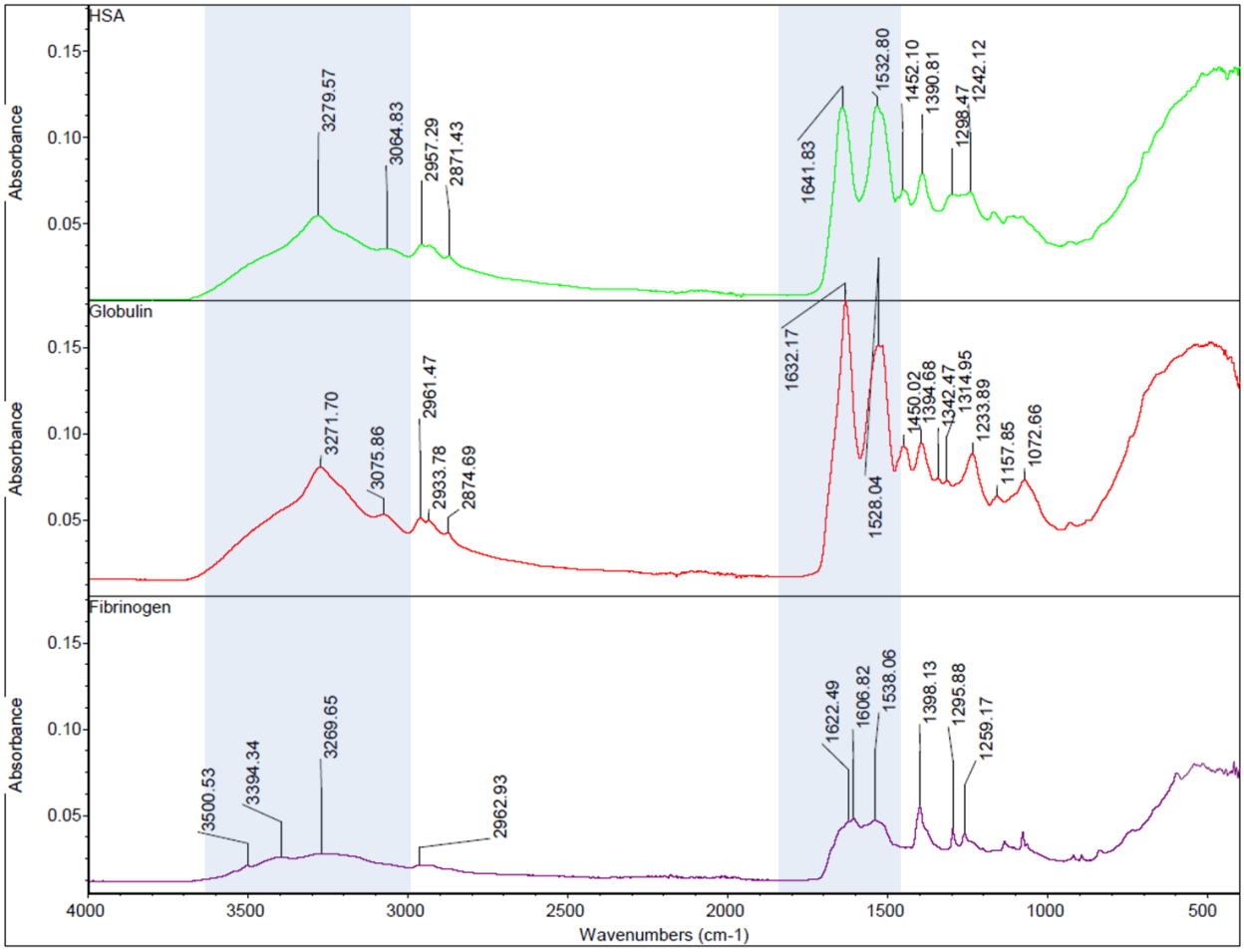

Figure 3.11. FTIR spectra of pure proteins in its powder form

As explained in **Section 2.2.2**, three sets (one for each protein) with four samples were used for static protein adsorption test: 1-2) pristine membrane immersed in protein and just in PBS, 3-4) coated membrane immersed in protein and just in PBS.

FTIR spectra of coated membranes (denoted as PVDF PS-PAA in **figure 3.12)** exhibited peaks at 1601 and 1493cm^{-1} which is characteristic of the PS-PAA copolymer (**figure 3.1**) confirming successful coating of the surface. The samples immersed in proteins have peaks at 1650 and 1540cm^{-1} which are shifted but close to the peaks of pure proteins (**figure 3.11**). All three proteins have similar FTIR spectra due to the similarity of their composition. Also, protein peak height intensity adsorbed on pristine and coated membranes have little to no difference suggesting that the proteins have the same degree of interaction with the pristine and coated membranes.

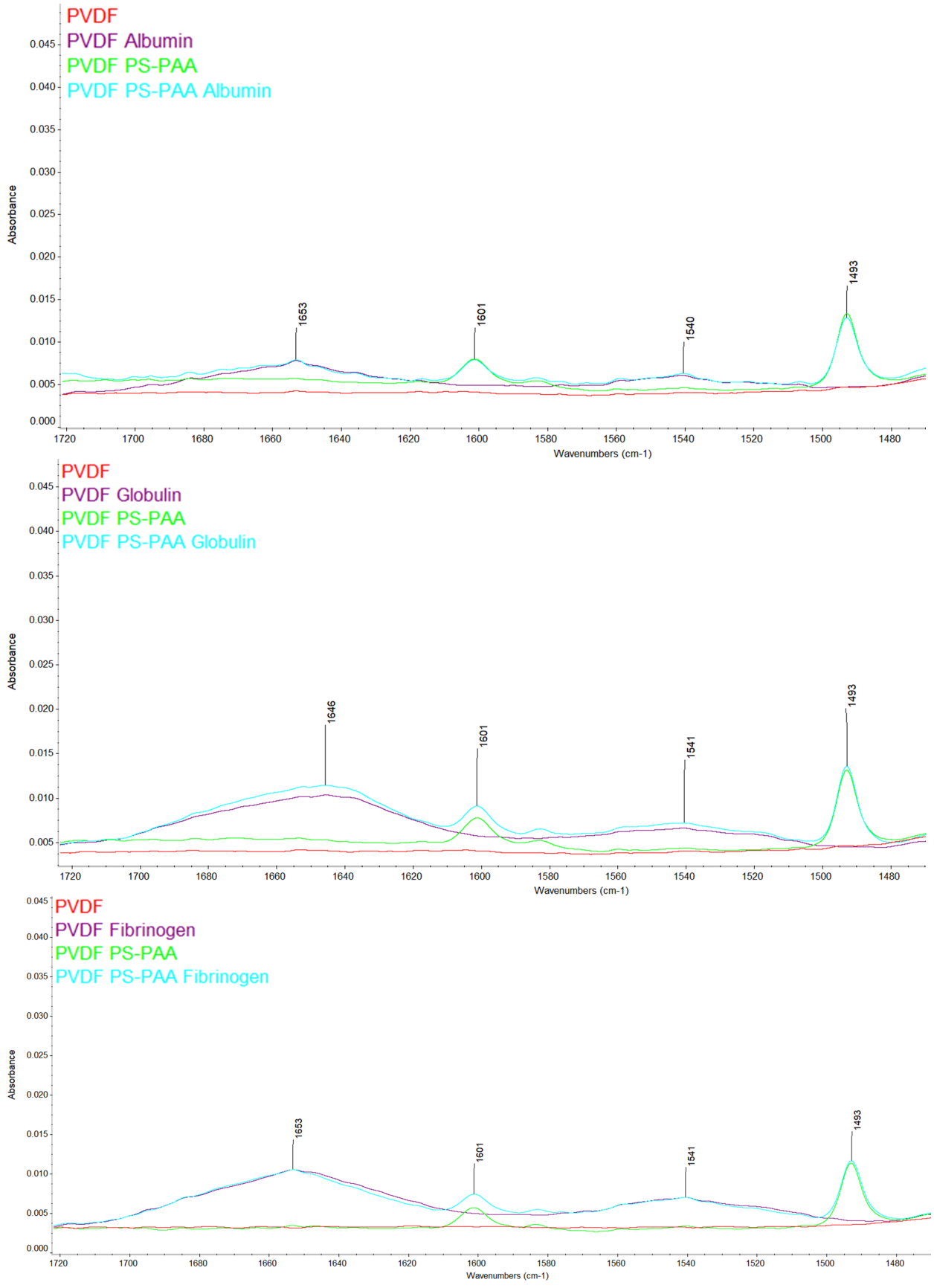

Figure 3.12. FTIR spectra of proteins adsorbed on pristine and coated membranes

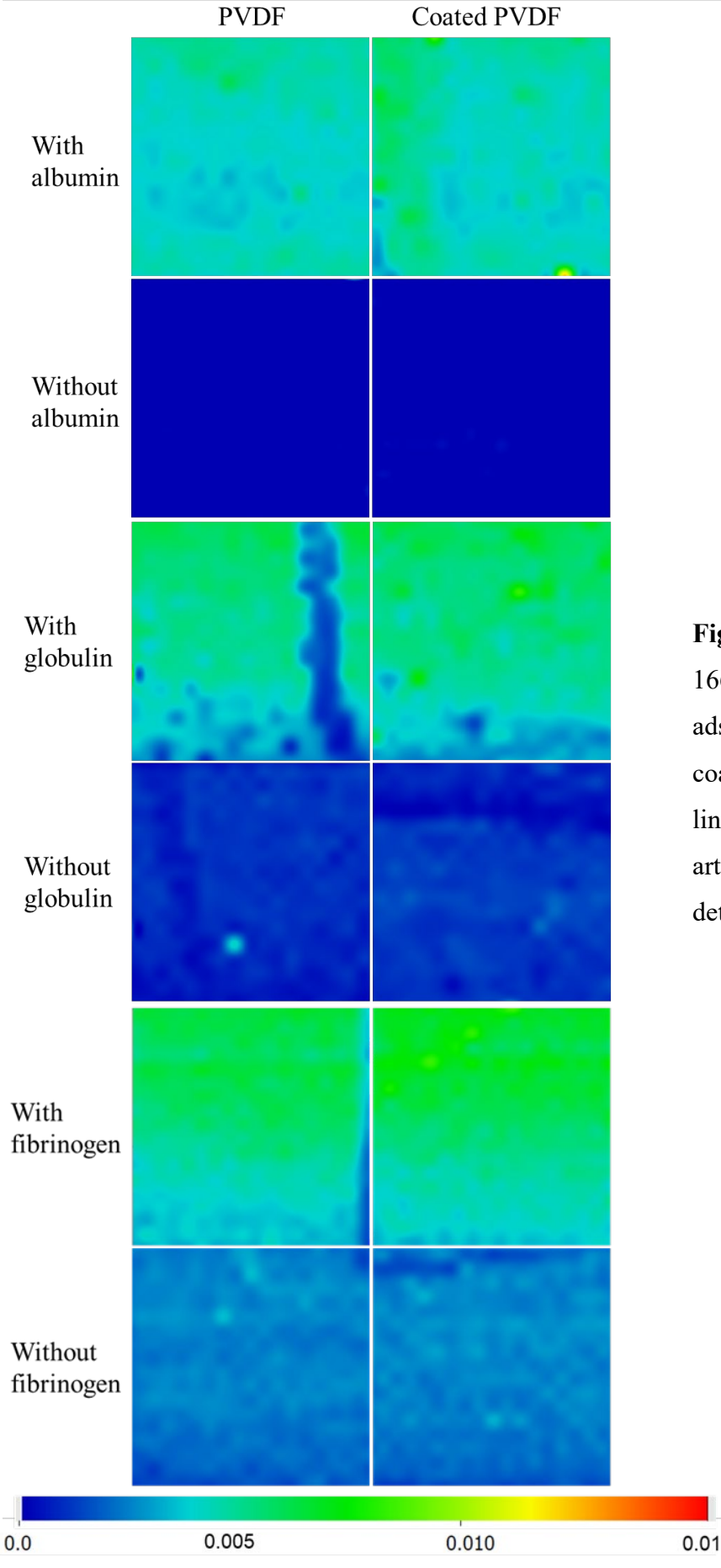

Figure 3.13. FTIR maps at 1660cm^{-1} of proteins adsorbed on pristine and coated membranes. The blue line in globulin mapping is an artifact caused by the detector.

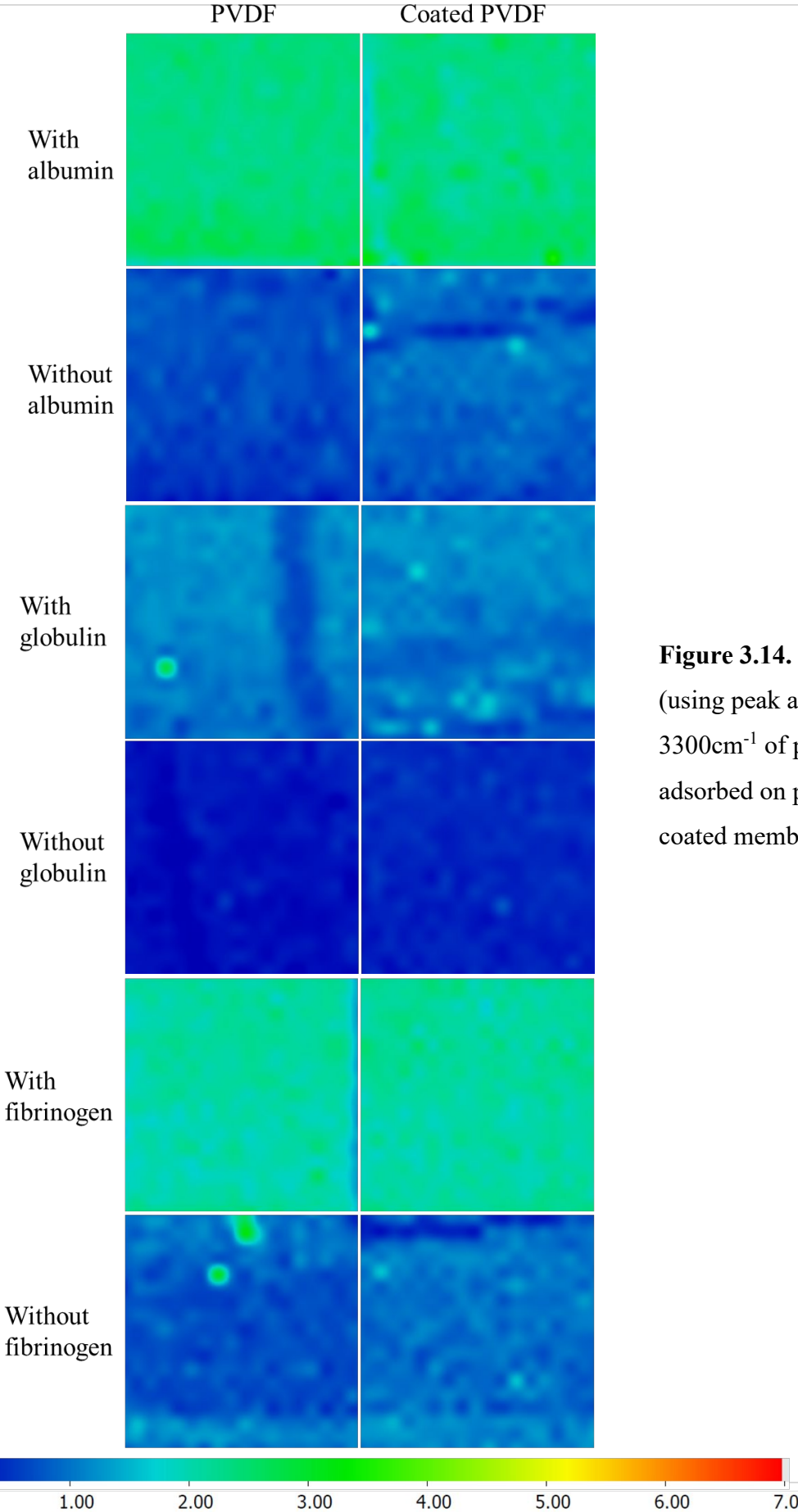

Figure 3.14. FTIR maps (using peak area) at 3300cm^{-1} of proteins adsorbed on pristine and coated membranes

The EM3E4SW Master is an Education Program supported by the European Commission, the European Membrane Society (EMS), the European Membrane House (EMH), and a large international network of industrial companies, research centers and universities (www.em3e-4sw.eu)

Figures 3.11 and **3.12** show that proteins have the strongest absorbance at around 1630 cm^{-1} and it does not overlap with the coating and membrane peaks. In FTIR mapping, the observable peaks are at 1660 which was used for the FTIR maps. Since a peak at 3300cm^{-1} is unique to the proteins, FTIR mapping at this peak was also conducted to verify the results. The chemical mapping of all the proteins (**figure 3.13** and **3.14**) and coating (**Section A.2.3 of Appendix**) confirm the results of the FTIR spectra. The proteins have the same adsorption on the pristine and coated membranes.

Some of the factors that could affect protein interaction with the copolymer are copolymer block chain length and its configuration, copolymer concentration, nature of the copolymer, and surface roughness. Studies of PS-PEGMA copolymer coating on PVDF membranes have shown that increasing the chain length of the hydrophilic PEGMA blocks increased its fouling resistance to proteins [18, 39]. Protein adsorption decreases with increasing PS-PEGMA copolymer concentration up to a certain concentration where there is no significant improvement of fouling resistance [33, 39]. Since protein adsorption on varied copolymer concentrations and surface roughness measurement were not conducted in this study, these factors could not be elaborated. However, it is known that the block copolymer, $(PS)_{275}$-b-$(PAA)_{30}$, is only 10 wt.% PAA and its PAA chain length is much smaller (DP=30) than the PS (DP=275). As discussed in **Section A.1.1 of the Appendix**, the small amount of PAA chains could have led to more coiled and isolated PAA structures (dilute regime) instead of forming extended brushes (semi dilute regime). The PAA chain is possibly too short and did not have the desired configuration to have a significant contribution to the interaction with proteins.

It would be interesting to identify which protein has the strongest interaction with the copolymer. However, different materials have different degree of absorption in FTIR although they have similar peaks. Thus, the FTIR absorption of the proteins could not be compared to each other. One possible characterization technique that can be used is UV-Visible spectroscopy. If the final protein concentration after immersion of the membranes could be measured using UV-Vis spectrophotometer, combining with the known initial protein concentration, it would be possible to evaluate the amount of protein adhered to the membrane.

4. CONCLUSION AND RECOMMENDATIONS

This study intends to optimize the coating procedure of PVDF membrane using $(PS)_{275}$-b-$(PAA)_{30}$ copolymer as the surface modifier and investigate its interaction with major human blood proteins – albumin, ɣ-globulin, and fibrinogen.

A 5mg/mL copolymer concentration, 2h coating time, and drying the coating before washing are the optimum process conditions identified to obtain a good $(PS)_{275}$-b-$(PAA)_{30}$ coating coverage on PVDF membrane. The pure water permeability decline due to the coating at 1mg/mL and 5mg/mL is minimal (6.15% and 11.8% respectively). However, the measured permeabilities do not completely follow Darcy's Law which could be due to the unswelling of membranes with increasing pressure or to residual compaction occurring at high pressure. Thus, it is recommended to measure also the permeability from higher to lower pressure. All three human blood proteins have a similar amount of adsorption with the pristine and coated membranes which are attributed to the short PAA chains (only 10wt.% of the copolymer). The surface remained coated after water filtration.

For future studies, it is recommended to: 1) test other copolymers or use PS-b-PAA with longer PAA chains to observe its interaction with proteins, 2) investigate the effect of changing copolymer concentration and hydrophobic/hydrophilic block ratio on protein interactions, 3) determine the protein with the strongest interaction with the copolymer (possibly using UV-Visible spectroscopy) or evaluate the competitive adsorption of the three proteins using fluorescence microscopy, and 4) conduct filtration tests with protein solution to identify the selectivity of the membrane towards each protein and evaluate fouling. The use of other characterization techniques might also provide some additional insights. SEM could confirm if there were structural changes to the membrane after coating. AFM could also determine the modified membrane's surface roughness and potentially its hydrophilicity (ie. quantifying the interaction between a surface and a probe such that a hydrophilic probe will have stronger interaction with a hydrophilic surface than a hydrophobic surface) which could affect the protein adsorption on the coating.

APPENDIX

A.1. BIBLIOGRAPHIC STUDY

A.1.1 COATING

Coating by immersion is an interesting membrane surface modification technique due to its simplicity and scalability. It only involves two steps: 1) immersion of the membrane in the coating bath (copolymer solution) for a specific time followed by 2) drying to remove residual solvent. The formation of hydrophilic polymer brush on a surface is related to its density on the surface, σ (**equation A.1**) [40]. Although the following discussion was initially used on grafted hydrophilic polymers, it can also be helpful in understanding the behavior of coated polymers on a surface. When grafting density becomes larger than a threshold value, σ_{th} (**equation A.2**), the behavior of the polymer brushes changes from dilute regime to semi-dilute regime (**figure A.1**). The semi-dilute regime favors steric repulsions which prevents colloids (or proteins) adhesion.

$$\sigma = \frac{a^2}{D_b^2} \qquad \textbf{(equation A.1)}$$

$$\sigma_{th} = N^{-\frac{6}{5}} \qquad \textbf{(equation A.2)}$$

where a is the monomer dimension, D_b is the distance between the polymer chains, and N is the number of monomers per chain. The threshold value is only dependent on N.

The equilibrium polymer brush length, L_o, is given by **equation A.3** where k_1 and k_2 are osmotic and elastic proportionality constants, respectively [41].

$$\frac{L_o}{Na} = \left(\frac{5k_1}{7k_2}\right)^{1/3} \sigma^{1/3} \qquad \textbf{(equation A.3)}$$

However, **equation A.3** is only valid in semi-dilute regime and for very long polymer chains [42]. From this equation, brush length is only a fraction of the polymer length implying that

the chains are not fully stretched. On the other hand, volume fraction of the polymer in the brush is given by,

$$\phi = \frac{Volume\ of\ polymer}{Volume\ of\ brush} = \frac{Na^3}{L_o D_b^2} = \frac{Na}{L_o}\sigma \qquad \textbf{(equation A.4)}$$

Combining **equation A.3** and **A.4**,

$$\phi = \left(\frac{5k_1}{7k_2}\right)^{-1/3} \sigma^{2/3} \quad \textbf{(equation A.5)}$$

From these equations, polymer brush length and volume fraction occupied by the polymer within the brush are dependent on grafting density. Increasing grafting density beyond the threshold value results in increase of L_o and ϕ. Thus, these suggest that factors affecting coating density should be considered. Also, the effect of the hydrophobic chain should be investigated since it was not taken into account in this model.

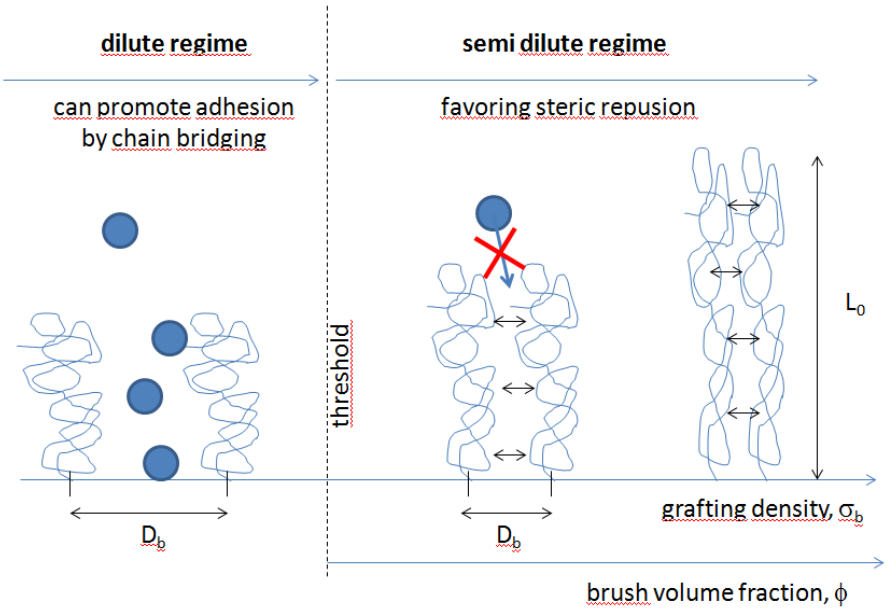

Figure A.1. Hydrophilic polymer regimes when grafted on a surface [40]

Since coating relies on non-covalent interactions between the coating and the membrane surface for efficiency and stability, the coating amount depends on the extent of interaction between the two which can be influenced by the nature of the copolymer coating (polymer chain length, hydrophobic/hydrophilic block ratio, configuration) and process conditions (coating time, polymer concentration, solvents used).

A.1.1.1 EFFECT OF HYDROPHOBIC/HYDROPHILIC BLOCK RATIO OR CHAIN LENGTH

Self-assembly of a copolymer on a membrane surface can be optimized by controlling the copolymer's hydrophobic/hydrophilic block ratio and the block's molecular size or chain length. Studies of PS-PEGMA copolymer coating on hydrophobic PVDF membranes have shown that increasing the chain length of the hydrophilic PEGMA blocks reduced copolymer adhesion [18, 39]. An increase in chain length of PEGMA while keeping the chain length of PS anchoring block constant (also decrease in PS/PEGMA ratio) decreased the adsorbed coating and required copolymer coating concentration (**figure A.2**) [39]. This means that larger PEGMA moieties introduced increased steric hindrance blocking the access of PS moieties to the PVDF surface.

Venault *et al.* [43] coated PVDF membranes with a block copolymer of poly(propylene oxide) and poly(sulfobetaine methacrylate) (PPO-b-PSBMA) to improve its blood compatibility. PPO was used as an anchoring block since it has a high tendency to establish hydrophobic interactions with any hydrophobic membrane material. PPO block length was kept constant while PSBMA chain length was varied. The highest coating density was obtained at the lowest PSBMA/PPO ratio (0.5) where PSBMA had the shortest length (**figure A.3**). It was attributed to two factors. First, when the PSBMA segment is relatively short, hydrophobic interactions between the PVDF membrane and PS dominates over hydrophilic interactions between the solvent and PSBMA segment. Conversely, when the PSBMA segment is long (PSBMA/PPO ratio=1 and 2), hydrophilic interactions become stronger since more PSBMA is available. As a result, it diminishes the coating efficiency driven by hydrophobic interactions. Second, similar to the previous study, longer hydrophilic PSBMA chain length increases steric hindrance. Also, it can be observed that the effect of PSBMA chain length on coating density is not linear (**figure A.3**).

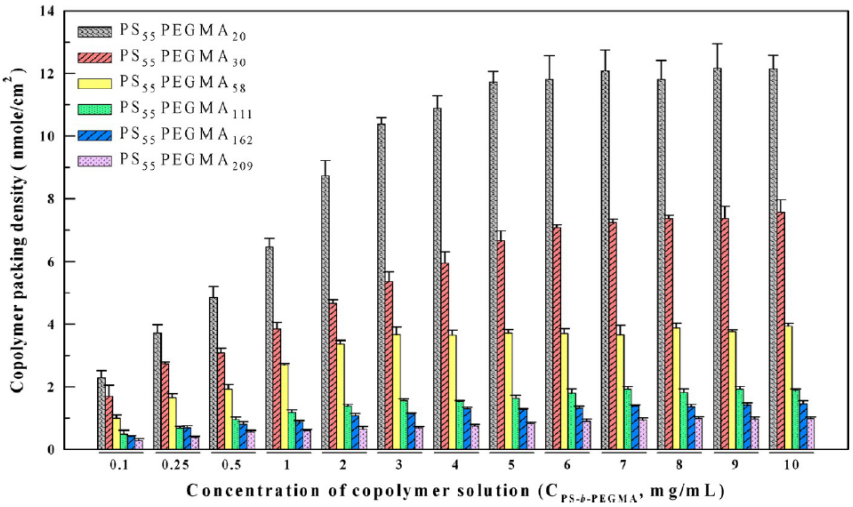

Figure A.2. PS-b-PEGMA coating density on PVDF membrane vs concentration of copolymer solution used as coating bath for different PS/PEGMA ratio [39]

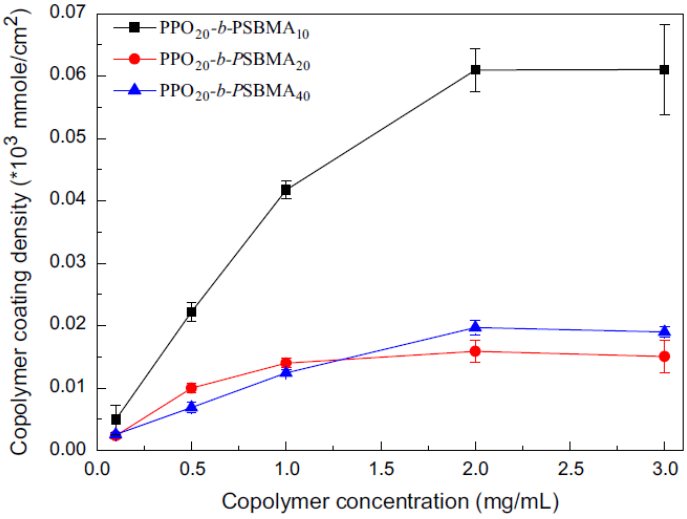

Figure A.3. Effect of varying PPO/PSBMA ratio and copolymer concentration [43]

These results were also correlated with surface roughness (**table A.1**). A lower root mean square (RMS) value means the surface is smoother. As mentioned earlier, membrane coated with PPO_{20}-b-$PSBMA_{10}$ exhibited the highest coating density. It also had the lowest RMS and was smoother than the uncoated membrane. This could indicate homogeneous coating as a result of less hindered and stronger hydrophobic interactions. Roughness increased when PSBMA chain length was increased indicating less homogeneous coating coverage as a result of stronger hydrophilic interactions disrupting the coating process.

Table A.1. RMS coefficients of PVDF membranes coated with PPO-b-PSBMA [43]

Copolymer	RMS (nm)
No coating	168.3
PPO_{20}-b-$PSBMA_{10}$	128.1
PPO_{20}-b-$PSBMA_{20}$	160.4
PPO_{20}-b-$PSBMA_{40}$	178.4

In another study using combined polymerization and coating process, PVDF membrane surface was modified with a random copolymer of PS and PSBMA (PS-r-PSBMA) to improve its anti-fouling properties [44]. PS/PSBMA ratio was varied where fibrinogen adsorption was used as an indication of coating efficiency instead of coating density. Results showed that at high hydrophilic block amount (70 to 100% PSBMA), there was high fibrinogen adsorption implying that it was difficult to establish hydrophobic interactions between the PS block and PVDF surface. This could mean that there was an insufficient coating amount.

These studies show that an increase of hydrophilic block does not improve coating density. Thus, these two factors must be minimized to achieve good coating coverage: 1) hydrophilic interactions between the solvent and copolymer, and 2) steric hindrance caused by hydrophilic block.

A.1.1.2 EFFECT OF COPOLYMER CONFIGURATION

Copolymer configuration also plays a role in coating adhesion. Yeh *et al.* [45] studied the effect of varying PS-PEGMA copolymer configuration (diblock, triblock, random) with similar copolymer molecular weights and hydrophilic/hydrophobic block (PS/PEGMA) ratio on coating density of PS surfaces. The random copolymer has the highest coating density, followed by diblock, then triblock. This is attributed to the random arrangement of the styrene units in the random copolymer which provided the most anchoring configurations to the PS surface than diblock and triblock copolymers assuming there are no chain repulsion and minor steric hindrance (**figure A.4**). Also, it is possible to have multilayer coating in random copolymer since the hydrophobic blocks are not completely in contact with the PS surface and the available PS blocks can have intra- and intermolecular interactions leading to multilayer coating.

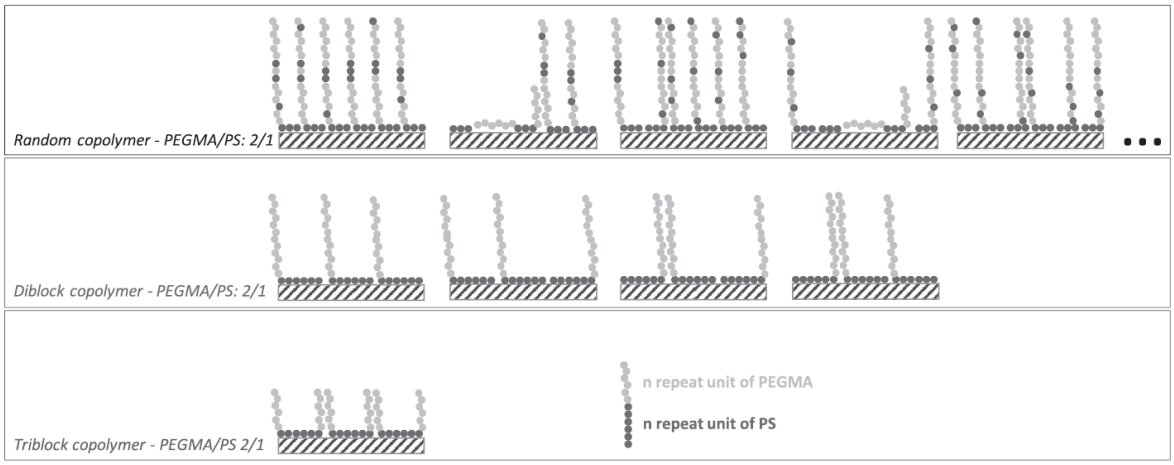

Figure A.4. Proposed assembly combinations of random, diblock and triblock PS-PEGMA copolymers on PS surface with PEGMA/PS ratio of 2/1 [45]

A similar trend in coating density was found when varying PS-PEGMA copolymer configurations were used to coat PVDF membranes [18]. Also, the random copolymer has a higher coating density than diblock copolymer whether it has a higher or lower molecular weight than diblock copolymer (**figure A.5**).

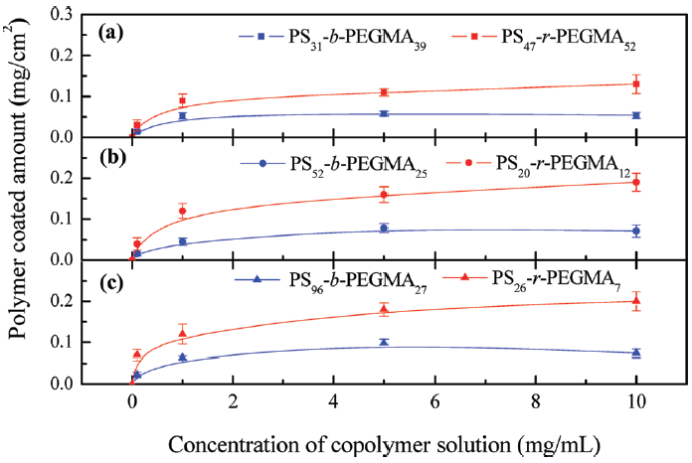

Figure A.5. Block and random PS-PEGMA coating density on PVDF membrane vs concentration of copolymer solution for a) PS/PEGMA ratio = 0.8-0.9, b) PS/PEGMA ratio = 1.7-2.1, and c) PS/PEGMA ratio = 3.7-3.9 [18]

Another study by Benavente *et al.* [33] using Fourier Transform Infrared Spectroscopy (FTIR) mapping to identify PS-PEGMA coating presence and to analyze its heterogeneity on

The EM3E4SW Master is an Education Program supported by the European Commission, the European Membrane Society (EMS), the European Membrane House (EMH), and a large international network of industrial companies, research centers and universities (www.em3e-4sw.eu)

PVDF membranes showed a different trend than the previous studies. Results showed that diblock copolymer had a better coating coverage level than random copolymer at lower copolymer concentrations (1 and 5mg/mL) but similar at a higher concentration (10mg/mL). Also, diblock copolymer had slightly better anti-adsorption properties than random copolymer at lower concentration (1mg/mL) but similar at 5 and 10 mg/mL. The difference in the trend from the first study could be due to different surfaces used. The first study used PS surfaces which have stronger interaction with the copolymer than PVDF surfaces due to hydrophobic interactions between two groups of the same chemical nature. The second study used PEGMA blocks that were shorter or almost similar chain length with PS blocks (**figure A.5**) while Benavente *et al.* used PEGMA block twice longer than PS block (PS_{53}b-$PEGMA_{124}$ and PS_{61}-r-$PEGMA_{121}$). As mentioned earlier, long PEGMA brushes could introduce steric hindrance minimizing its coating efficiency.

A.1.1.3 EFFECT OF COPOLYMER CONCENTRATION

Copolymer concentration should also be considered in optimizing the coating process. Studies have shown that coating density increases with PS-PEGMA copolymer concentration until it reaches a plateau regardless of the copolymer configuration [33, 45]. However, as stated earlier and presented in **figure A.2**, the hydrophobic/hydrophilic segment ratio also plays a significant role in coating concentration efficiency [39].

In another study [46], PVDF membranes were coated with zwitterionized and unzwitterionized poly(styrene-r-4-vinylpyridine) (**figure A.6**) with varying concentration to investigate the random copolymer's anti-fouling properties. Results showed that coating density increased with copolymer concentration until a plateau was reached at larger concentrations (10mg/mL) which could be an indication of the saturation of the interface. However, lower coating densities were observed for zwitterionized than unzwitterionized membranes despite having similar coating concentrations. This implies that coating efficiency also relies on the two opposing forces: 1) non-polar interactions between the hydrophobic anchoring block of the copolymer and membrane's surface, and 2) polar forces between the hydrophilic block of the copolymer and coating solvent. Zwitterionized membranes can have stronger hydrophilic or polar interactions with the solvent (**figure A.6**), thus, destabilizing the coating and resulting in lower coating efficiency.

Using combined polymerization and coating process, PVDF membrane surface was modified with PS-r-PSBMA and the copolymer concentration was varied [44]. Instead of coating density, fibrinogen adsorption and water contact angle (WCA) were used as indicators of coating efficiency. Measured WCA and fibrinogen adsorption decreased with increasing concentration until it reached a plateau implying the potential increase of coating on the surface until it reached saturation. In another study where they coated PVDF membranes with PPO-b-PSBMA showed a similar trend (**figure A.3**) where coating density increases with copolymer concentration and eventually reaches a plateau [43]. The results of these studies suggest that the occurrence of plateau or saturation is common. This is because at higher concentration, the surface may be fully covered, and the copolymers already attached to the surface may prevent the copolymers in the solution to reach the surface and be attached to it. Thus, copolymer concentration should be optimized when designing a coating process to avoid the excess use of coating material.

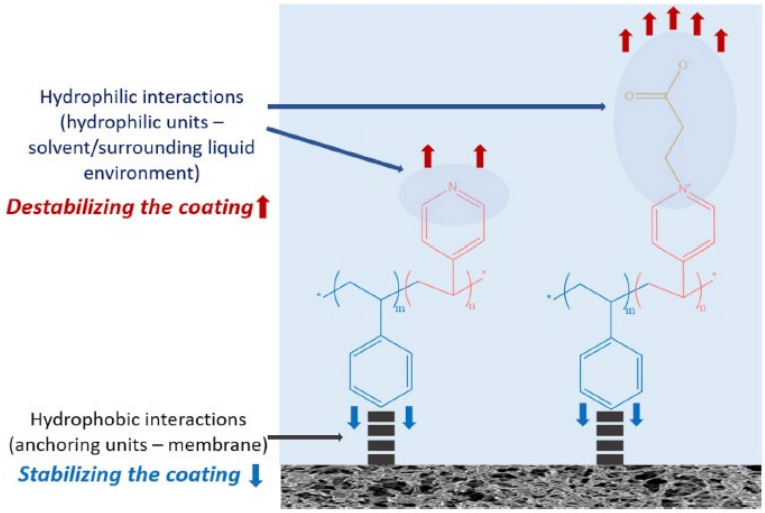

Figure A.6 Interactions of the unzwitterionized (left) and zwitterionized (right) copolymers with the aqueous environment [46]

A.1.1.4 EFFECT OF COATING TIME

Optimization of coating time is rarely discussed in bibliographies related to membrane coating. Researchers usually specify coating time without further explanation as to why that time was used. Intuitively, an increase in coating time should lead to a more coating amount

since the copolymers are given enough time to self-assemble on the surface. This was confirmed by Benavente *et al.* [33] when they coated PVDF membranes with PS-PEGMA copolymers. Senusi *et al.* [47] used tannic acid and tetraethylenepentamine to coat PVDF membranes for emulsion oil/water separation. Varying coating time from 2 to 12h showed an increase in deposition degree until it reached a plateau at 7h. Similarly, an increasing trend with plateau was also observed when PVDF membrane was coated with PS-r-PSBMA [44]. These studies suggest that the self-assembly process reaches a saturation point at longer coating time. Similar to the effect of high coating concentration, the copolymers in the solution need to overcome the barrier created by the already attached copolymers. Consequently, coating becomes less and less favorable as coating time increases. Thus, optimum coating time should be established.

A.1.1.5 COATING STABILITY TESTS

Although an optimum coating amount has been established, it is also necessary to conduct stability tests to confirm its potential in the desired application. In one study [39], PS_{55}-b-$PEGMA_{30}$ and PS_{94}-b-$PEGMA_{51}$ with molecular weights above 20kDa and PS/PEGMA ratios of 1.86 remained stable for 60 days on PVDF membrane when immersed in pure water. Also, when PS_{55}-b-$PEGMA_{30}$ was tested under regular chemical cleaning with citric acid, NaOCl, and NaOH solutions with ultrasonic treatment up to 6h, only less than 5% of coating was washed away. In another study [18], less than 10% of the PS-PEGMA copolymer was removed on PVDF membranes after 30 washes of pure water. Stability of coated poly(styrene-r-4-vinylpyridine) on PVDF membranes was also tested by immersing it in a 1M NaOH bath and 1M HCl bath for one week each [46]. Results showed that a large amount of copolymer remained coated on the PVDF surface. PVDF membrane modified with PS-r-PSBMA also remained stable when immersed in PBS for 7 days [44]. Thus, the use of PS as an anchoring block on the PVDF surface could be promising for this study.

A.1.2 CHARACTERIZATION

It is essential to determine the modified membrane's surface properties (chemical composition, surface wettability, and morphology) through surface characterization to understand its performance and stability. There are numerous characterization methods which can be divided into groups – spectroscopic techniques for surface chemical analysis, contact angle measurements for determination of membrane's wettability, microscopy techniques for analysis of surface morphology, and characterization of surface charge [30].

A.1.2.1 QUANTIFICATION OF MEMBRANE COATING AND FOULANTS

Coating density

Several studies [18, 33, 39, 43, 46] quantified the amount of coating on a membrane surface using coating density. It is done by measuring the weight difference between the modified, W_M, and unmodified, W_D, dry membranes with respect to membrane surface area, $A_{membrane}$ (**equation A.6**).

$$Coating\ density = \frac{W_M - W_D}{A_{membrane}} \qquad \textbf{(equation A.6)}$$

Although this method is fast and simple, it is not a very sensitive method as demonstrated by Benavente *et al.* [33]. Results showed that coating density started to plateau at copolymer concentrations beyond 3-5mg/mL but FTIR imaging showed that there was still an observable difference between 5 and 10mg/mL concentration. Also, this method cannot verify the homogeneity of the coating. It does not consider the contribution of the pores to the surface area and the amount of coating that penetrates the pores during coating. Lastly, membranes could potentially absorb moisture when exposed to air which could lead to overestimation of the measured weights. Thus, it is recommended to consider the coating density trend instead of the actual value [33].

UV Visible spectroscopy

UV Visible spectroscopy is an analytical technique where a sample is irradiated with light of different wavelengths in the visible, ultraviolet, and near-infrared regions [48]. Depending

on the content of the sample, the light is partially absorbed. The remaining transmitted light will be detected and recorded as a function of wavelength creating the sample's UV Vis spectrum which can be used to identify or quantify the content of the sample. Generally, the results are presented as absorption as a function of wavelength since the intensity of the absorption is directly proportional to the concentration of the analyte. Also, the concentration can be obtained quantitatively by measuring absorptions of multiple standard solutions with known concentration followed by the application of Beer-Lambert's Law.

Yeh *et al.* [45] determined the amount of PS-PEGMA copolymer coated on PS surfaces by measuring the copolymer concentration left after the coating process using a UV Vis spectrophotometer at 220nm. Since the initial copolymer concentration is known, the difference in concentration before and after the immersion is the amount adsorbed on the PS surface. Some researchers [39, 43] used UV Vis spectrophotometer to quantify the adsorbed BSA and lysozyme on PVDF membranes. The remaining concentration of the protein on the solution after the immersion process was determined by measuring the absorbance at 280nm. However, this method does not consider the amount of coating that penetrated the pores.

A.1.2.2 MEMBRANE SURFACE CHEMICAL ANALYSIS

Determination of the membrane's surface chemical composition is essential to verify the the presence of coating and adsorbed foulants. Their amount can be correlated to assess the modified membrane's performance and stability. There are numerous characterization techniques for this purpose as summarized in **table A.2**. However, it should be considered that membranes are generally used in their wet state while some characterization techniques only allow analysis using samples in its dry state. Thus, it is important to keep in mind that membranes could behave differently depending on the characterization technique used.

Table A.2. Spectroscopic methods used in membrane surface characterization [29]

	Infrared Spectroscopy (IR)	Raman Spectroscopy	Energy Dispersive X-ray Spectroscopy (EDS)	X-ray Photoelectron Spectroscopy (XPS)
Detection of elements	No	Yes	Yes, Be-U	Yes, H-U
Detection of functional groups	Yes	Yes	No	No
Detection of chemical bonds	Yes	Yes	No	Yes
Determination of crystallinity	Yes	Yes	No	No
Qualitative analysis	Yes	Yes	Yes	Yes
Quantitative analysis	Yes	Yes	Yes	Yes
Mapping/imaging of the chemical composition possible	Yes	Yes	Yes	Yes
Depth profiling of the chemical composition possible	Yes	Yes	No	Yes
Analysis in vacuum	No	No	Yes	Yes
Wet samples can be analyzed	No	Yes	No	No
Special sample pretreatment	No	No	Yes	No
Sample destructive technique	No	Yes/No	Yes	No
Analysis depth	1–100 μm (PAS) 1–10 μm (ATR)	1–5 μm	0.5–5 μm	1–3 nm
Spatial resolution	0.5–1 μm (ATR, PAS)	0.5–1 μm (confocal Raman)	0.5–5 μm	5–50 μm
Detection limit	1 atom% (ATR)	[a]	0.1 atom%	1 atom%

[a] A general value is not available because the detection limit depends strongly on the equipment and the measuring conditions.

In infrared (IR) spectroscopy, the sample is irradiated with infrared light. When the frequency of the incident light matches the vibration of the molecules in the sample, the molecules absorb the radiation. The remaining transmitted light is detected and converted to a spectrum showing the changes in the infrared intensity as a function of frequency (or wavenumber). The peaks in the spectrum correspond to bond stretching or deformation specific to functional groups present in the sample and its intensity could be correlated to the amount.

Raman spectroscopy uses a monochromatic light source which can be in UV, visible, or near-infrared regions. This technique uses the concept of Raman scattering to generate a spectrum with intensity of the scattered light as a function of Raman shift (energy difference between the incident and Raman scattered photons). Groups with double and triple C-C bonds, disulfide bonds, and C-H bonds are detected easily with Raman spectrometer, while it is the opposite for water [29]. Consequently, this is interesting for membrane characterization as it allows analysis of wet samples. Raman spectroscopy is complementary to FTIR since bands that are strong in infrared spectrum are weak in Raman spectrum and vice versa [29, 30].

In X-ray Photoelectron Spectroscopy (XPS), the sample is placed under ultrahigh vacuum and is irradiated with focused X-rays resulting in photoemissions. The emitted electrons and their binding energies unique for each element will be detected allowing identification of the elements present in the sample. Results are presented as spectrum with intensity as a function of binding energy. Also, the peak intensity is proportional to the quantity of the element in the sample. This method is non-destructive and non-conducting samples, such as polymeric membranes, can be analyzed without conductive coating. However, the membranes should be analyzed in their dry state, and the analysis time should be kept short since increased exposure period could lead to sample deterioration [29].

Energy-dispersive X-ray Spectroscopy (EDS) is coupled with an electron microscope where the sample is irradiated with an electron beam followed by X-ray generation which is unique for each element. However, this technique requires that the sample chamber is under vacuum condition, thus, membranes must be analyzed in their dry state. Also, non-conducting samples, such as polymeric membranes, should be coated with a conductive material prior to the analysis. There is also a possibility of alteration in the composition of polymeric samples upon exposure to the electron beam [29].

Fluorescence Microscopy

When multiple proteins are present on a sample surface, FTIR technique may not be able to distinguish them from one another due to their almost similar composition. For this reason, fluorescence microscopy is useful. It uses laser of a specific wavelength as the incident light source which will excite the fluorescent molecules or fluorophores in the sample. The sample will then emit fluorescent light of another wavelength in which the observer can view through the fluorescent microscope. This method can visualize autofluorescent specimens on a surface. For samples that have either extremely faint or bright, nonspecific fluorescence, they can be attached with fluorescent stains or fluorescent-tagged antibodies. This technique is capable of detecting a single molecule. Using multiple fluorescence labeling and different probes, it can also simultaneously identify several target molecules. Thus, fluorescence microscopy could be advantageous in this study to observe the competitive adsorption of HSA, globulin, and fibrinogen on the modified membrane surface.

Fluorescence microscopy was already used to investigate the static adsorption of fluorescein isothiocyanate labeled BSA (BSA-FITC), and fluorescent stained *E. coli* and *P. putida* on modified polyvinyl chloride (PVC) membrane [49]. The fluorescent intensity was detected by a confocal laser-scanning microscope (CLSM) and the relative fluorescent intensity was calculated by ImageJ software. Also, it can be coupled with specifically designed microfluidic chips to quantify proteins [50] or observe fouling and filtration behavior at the same time [51, 52].

A.1.2.3 MEMBRANE'S WETTABILITY

Surface wetting mostly governs the interactions between solid surfaces and fluids. Thus, this phenomenon is essential when investigating membrane processes since it influences flux, rejection, and fouling [30]. The most common method to determine the degree of wetting is through the measurement of the contact angle formed by a droplet of fluid on membrane's surface (**figure A.7**). It depends on the interfacial tensions of all the interfaces involved. For instance, when a drop of water is put on a solid surface under air, the shape of the drop changes under the pressure of the different surface-interfacial tensions until equilibrium is reached. A hydrophilic surface will favor the interaction with water, thus, the water droplet spreads on the surface and the measured contact angle is small. Conversely, a hydrophobic surface will repel water, thus, to minimize their interaction, the contact angle formed will be high. It should be considered that the sample's contact angle could change depending on the environment implying that measured contact angles could be different for dry and wet states. For instance, polymeric membranes tend to reorganize their structure to adapt to the surrounding medium [53]. Consequently, its surface properties will vary depending on the environment it is currently in. Since membranes are generally used in their wet state, it would be more interesting to observe its surface wetting properties in an environment similar to its working condition that is their wet state. There are several methods to measure contact angle – sessile drop method, captive bubble/drop method, and Wilhelmy plate method [29, 30].

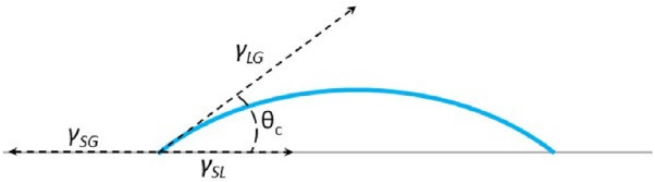

Figure A.7. Contact angle formed on a surface

Sessile drop method

In the sessile drop method, a droplet is placed on the sample surface using a syringe followed by digital measurement of the contact angle (**figure A.8**). This is the simplest method to assess membrane's wettability, however, the membrane sample should be in its dry state. Also, accurate contact angle measurements are difficult to achieve due to the non-ideality of the surface (surface roughness), varying ambient conditions (dry or humid atmosphere), and influence of impurities [53, 54]. Drying of samples before the analysis could also potentially alter the structure of membranes.

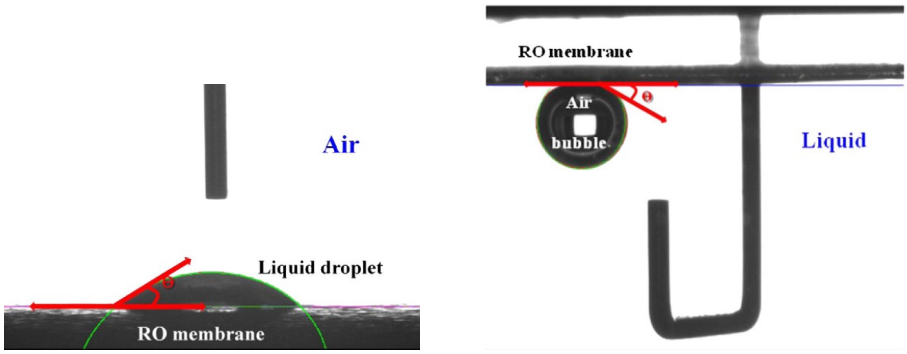

Figure A.8. Sessile drop (left) and captive bubble (right) methods [55]

Although several studies [33, 39, 43-47] used sessile drop method to assess membrane's wettability, Benavente *et al.* [33] showed that it is not a very sensitive method. The measured contact angles did not vary significantly even though the coating density increased. Zhang *et al.* [53] showed that different contact angles were measured for UF membranes dried at varying periods. Thus, one should ensure that the membranes are dried long enough to obtain more accurate results. Baek *et al.* [55] studied the effect of drying condition (ambient drying and vacuum oven drying), measurement time, and droplet volume using commercial polyamide RO membranes. The experiment was conducted at the same time to minimize the effect of varying ambient conditions (humidity and temperature). The measured contact angle decreased with measurement time which was attributed to two reasons. First, the water droplet potentially altered the surface structure of the membrane by exposing its hydrophilic groups more. Second, the continuous spreading on the surface could have resulted in enhanced evaporation. With varying drop volume, no trend in the contact angle measurements was found, while up to 30^{o} difference in the contact angle values were found for membranes dried in ambient conditions

and 40°C in vacuum oven. However, drying at higher temperatures 40-80°C resulted in small variation (up to 4°). Also, results showed that there could be membrane damage due to the drying process. Combining this with the findings of Zhang *et al.* [53], membrane sample preparation (drying length and temperature) plays a significant role in contact angle measurement using sessile drop method.

Captive bubble method

Surface wetting analysis of membranes on their wet state can be done through captive bubble method. Here, the membrane is suspended (asymmetric membranes are inverted with the active side facing down) and immersed in a liquid such as water (**figure A.8**). Using a J-shaped syringe needle, a bubble of air is introduced underneath the membrane's surface since air is less dense than water. It is also possible to use a droplet of fluid instead of air as long as it is immiscible to the ambient fluid [56]. This method overcomes some of the challenges in sessile drop method such as contamination and varying ambient condition. It minimizes contamination of the solid surface with air-borne impurities [54] since the air bubble rapidly gets saturated with water [53]. Also, there is no variation of contact angle through time since there is no evaporation of the droplet. Baek *et al.* [55] proved that contact angle using captive bubble method is indeed time-independent but it increased with air bubble volume which could be due to increased buoyancy force. In this method, there is also a possibility to adjust the temperature of the liquid to mimic the membrane's working condition. However, one should ensure the compatibility of the membrane with the ambient fluid such that it will not dissolve.

Zhang *et al.* [53] compared the results of two methods on different UF membranes. Results showed that both methods have comparable contact angles with statistical differences within acceptable ranges except for one membrane with a significant difference in advancing contact angle and time-dependent change in receding contact angle. The explanation provided is that this membrane changes its structure rapidly than the other membranes to adapt to the ambient liquid. Baek *et al.* [55] also compared the two methods on commercial polyamide RO membranes. **Table A.3** shows that contact angles from captive bubble method have close values for all polyamide RO membranes while results from sessile drop method varied from 18.3-71.2°. Researchers, therefore, concluded that the former method is more reliable and reproducible than the latter. However, it is also possible in captive bubble method that the

membrane surface is fully wetted by water and that the air bubble is in contact with water rather than the membrane surface resulting in similar and time-independepent contact angles. Meanwhile, the variation in the contact angles of sessile drop method could be due to different effects of the drying procedure on the different RO membranes.

Table A.3. Contact angles measured using sessile drop and captive bubble methods [55]

	SWC5	SW30HR	TM820	SHN	SHF	LFC-1	FLR
Sessile drop method[a]	38.2 ± 2.1	18.3 ± 0.8	27.5 ± 1.9	28.5 ± 2.1	71.2 ± 1.2	54.0 ± 3.3	34.6 ± 3.9
Captive bubble method[b]	40.6 ± 1.4	38.5 ± 1.0	39.0 ± 1.2	39.7 ± 1.0	37.2 ± 1.2	37.9 ± 0.8	39.1 ± 0.8

[a] Sessile drop method: measured with 6 μL of deionized water.
[b] Captive bubble method: measured with 10 μL of air bubble.

Wilhelmy plate method

In the Wilhelmy plate method, the membrane's contact angle can also be measured in its wet state wherein the membrane is fastened to a vertical rod and immersed edge-first in the liquid of known surface tension. However, this method requires that the sample is flat with regular geometry and identical properties in all planes. Thus, this method does not apply to asymmetric membranes [30].

A.2 SUPPLEMENTAL DATA FOR RESULTS AND DISCUSSION

A.2.1 OPTIMIZATION USING ETOH$_{ABS}$-THF MIXTURE AS THE SOLVENT

A.2.1.1 SOLVENT CHOICE

By visual inspection, PS-b-PAA does not dissolve completely in EtOH$_{abs}$. However, using 50%(v/v) EtOH$_{abs}$-THF as solvent resulted in the dissolution of the copolymer. To check if there is a difference in their coating efficiency, their FTIR spectra were obtained (**figure A.9**) using 3mg/mL copolymer concentration, 2h coating time, and IDW coating process. Results showed that the pristine membranes have similar spectra regardless of the solvent used. Also, coating with PS-b-PAA in EtOH$_{abs}$/THF solvent has higher peaks than EtOH$_{abs}$ solvent suggesting that proper dissolution of copolymer leads to more effective coating.

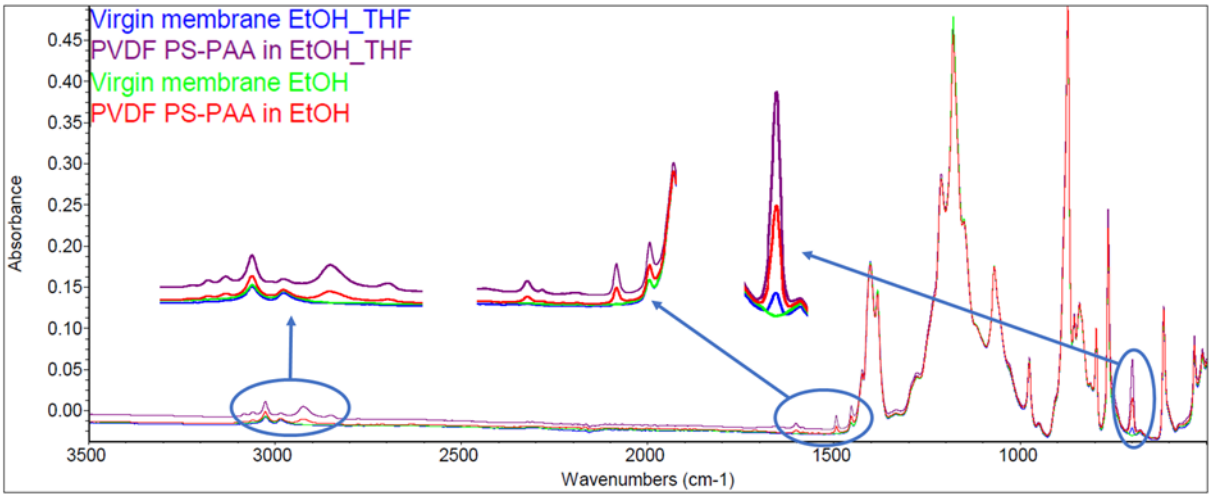

Figure A.9. FTIR spectra of pristine and coated membranes using EtOH$_{abs}$ and EtOH$_{abs}$/THF mixture as solvents

A study has shown that PVDF film immersed at pure THF for one week at 20°C did not dissolve [45]. However, it swelled and partly dissolved when immersed at THF at 60°C. Thus, it is important to consider working below this temperature when drying the membrane after immersion.

A.2.1.2 VARIATION OF OPERATING PROCESS

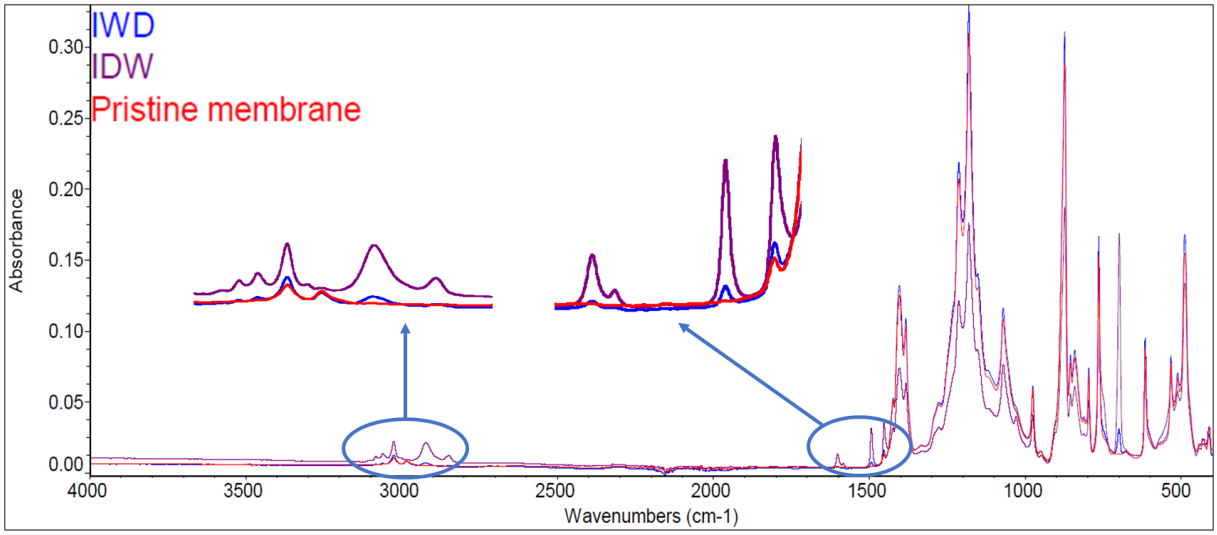

Figure A.10. FTIR spectra of pristine and coated membranes at different operating processes

A.2.1.3 VARIATION OF COATING TIME

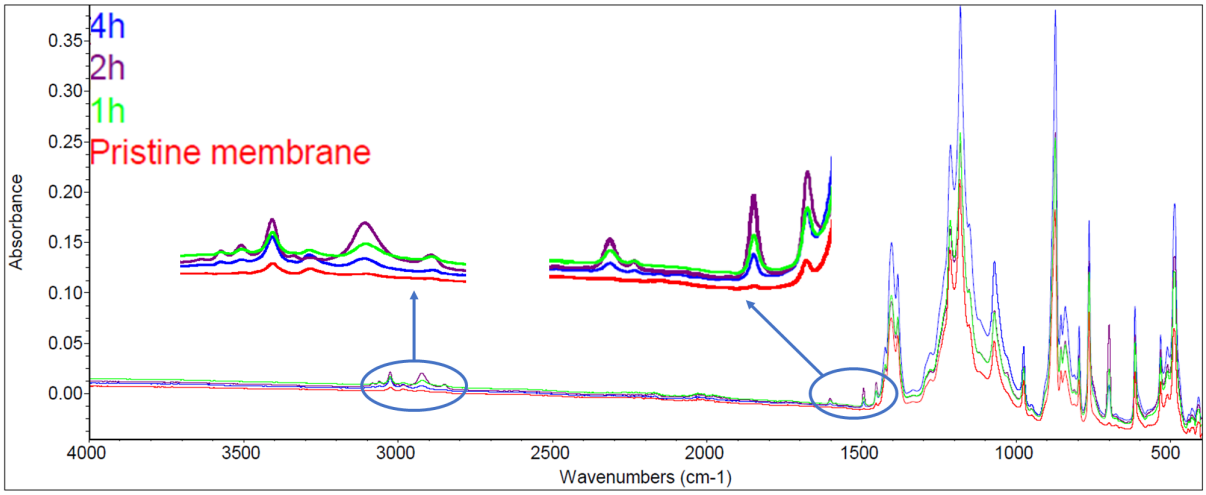

Figure A.11. FTIR spectra of pristine and coated membranes at varying coating time

A.2.1.4 VARIATION OF CONCENTRATION

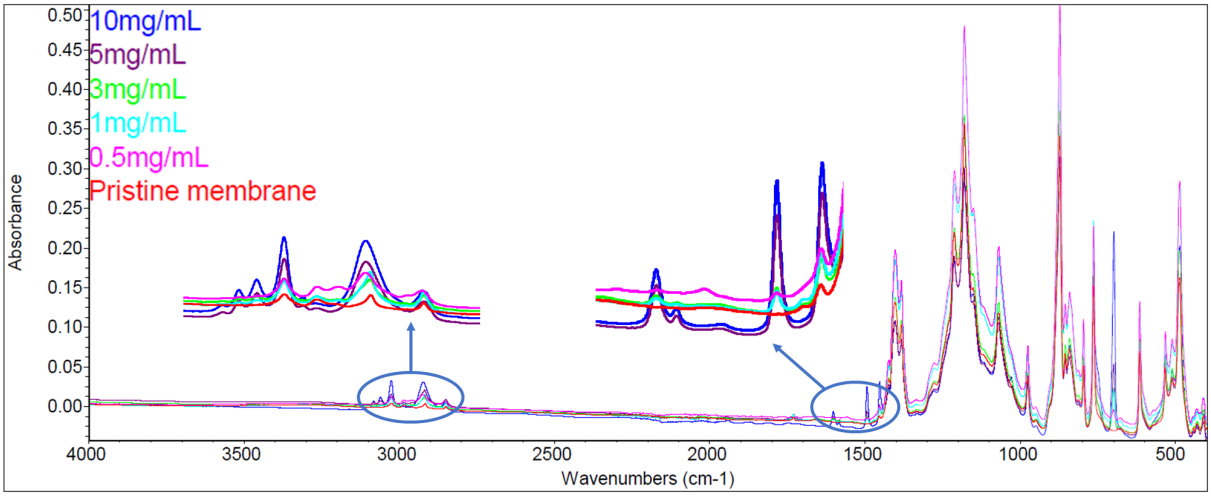

Figure A.12. FTIR spectra of pristine and coated membranes at varying copolymer concentration from 0.5 to 10mg/mL

A.2.2 PERMEABILITY MEASUREMENT

The weight of the permeate was measured every 5 minutes for four times. Flow rate, Q, was calculated by dividing the weight by 5 minutes.

Table A.4. Measured flow rate

	Pristine		Coated at 1mg/mL		Coated at 5mg/mL	
P (bar)	Weight (g)	Q (g/min)	Weight (g)	Q (g/min)	Weight (g)	Q (g/min)
0.2	0.950	0.190	0.810	0.162	0.870	0.174
	0.960	0.192	0.850	0.170	0.870	0.174
	0.950	0.190	0.830	0.166	0.860	0.172
	0.940	0.188	0.850	0.170	0.860	0.172
0.4	1.77	0.354	1.66	0.332	1.59	0.318
	1.77	0.354	1.65	0.330	1.56	0.312
	1.77	0.354	1.65	0.330	1.59	0.318
	1.77	0.354	1.65	0.330	1.57	0.314
0.6	2.48	0.496	2.41	0.482	2.25	0.450
	2.50	0.500	2.38	0.476	2.22	0.444
	2.49	0.498	2.42	0.484	2.22	0.444
	2.48	0.496	2.40	0.480	2.23	0.446

0.8	3.26	0.652	3.00	0.600	2.77	0.554
	3.20	0.640	3.01	0.602	2.78	0.556
	3.19	0.638	2.97	0.594	2.78	0.556
	3.13	0.626	2.99	0.598	2.78	0.556
1	3.71	0.742	3.53	0.706	3.34	0.668
	3.76	0.752	3.47	0.694	3.33	0.666
	3.72	0.744	3.46	0.692	3.32	0.664
	3.67	0.734	3.45	0.690	3.32	0.664
	3.69	0.738	3.45	0.690	3.30	0.660
	3.65	0.730	3.45	0.690	3.26	0.652
	3.64	0.728	3.45	0.690	3.24	0.648
	3.64	0.728	3.43	0.686	3.24	0.648
	3.59	0.718	3.40	0.680	3.25	0.650
	3.57	0.714	3.40	0.680	3.25	0.650
	3.57	0.714	3.40	0.680	3.24	0.648
	3.55	0.710	3.38	0.676		

A.2.3 VERIFICATION OF THE PRESENCE OF COATING USED IN THE STATIC PROTEIN ADSORPTION TESTS

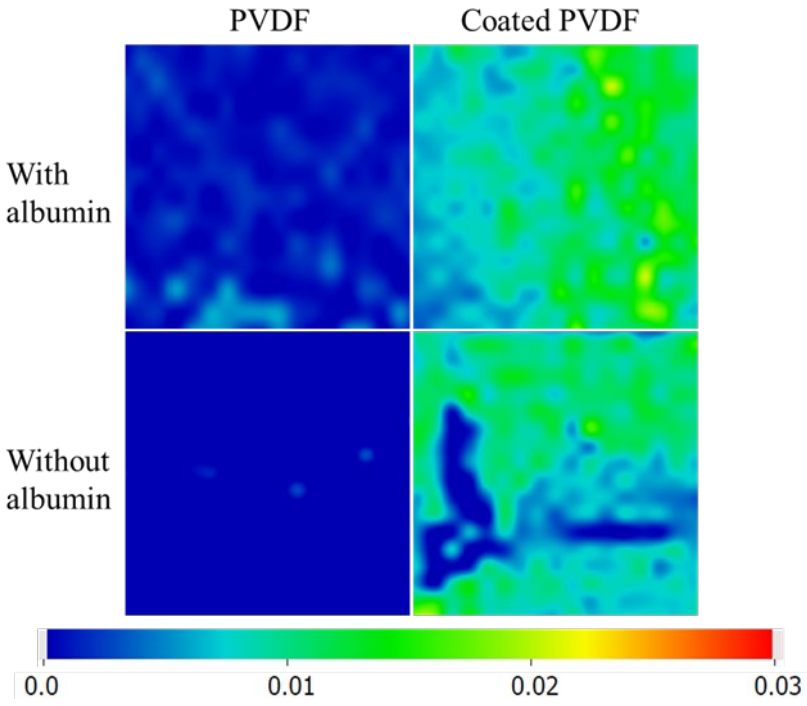

Figure A.13. FTIR maps at 700cm^{-1} to verify the presence of coating

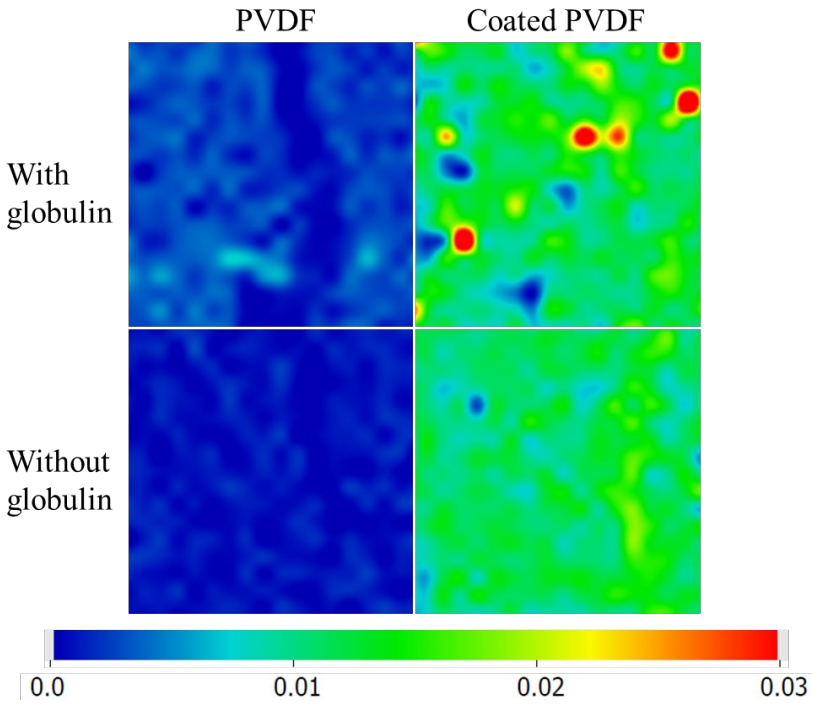

Figure A.14. FTIR maps at 700cm^{-1} to verify the presence of coating

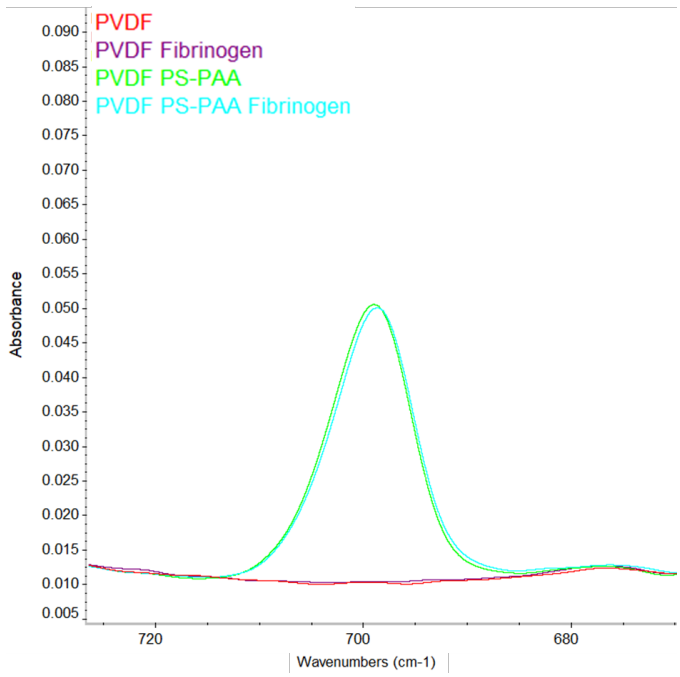

Figure A.15. FTIR spectra at 700cm^{-1} to verify the presence of coating

REFERENCES

[1] V. Laxmi, S. Tripathi, S. S. Joshi, and A. Agrawal, "Microfluidic Techniques for Platelet Separation and Enrichment," *J Indian Inst Sci,* Review vol. 98, no. 2, pp. 185-200, 2018, doi: 10.1007/s41745-018-0072-6.

[2] A. Venault, C. C. Yeh, N. T. Hsieh, and Y. Chang. *Smart Biomedical Membranes for Blood Separation, RSC Smart Materials*, vol. 2019-January, pp. 389-413, 2019.

[3] R. Hirano, K. Namazuda, J. Suemitsu, T. Harashima, and N. Hirata, "Plasma separation using a membrane," *Transfusion and Apheresis Science,* vol. 56, no. 5, pp. 649-653, 2017/10/01/ 2017, doi: 10.1016/j.transci.2017.08.008.

[4] D. Braile, A. Lima-Oliveira, A. Camim, R. Kawasaki-Oyama, and G. Sandoval, "Technological evolution of membrane oxygenators," *Brazilian Journal of Cardiovascular Surgery,* vol. 20, 12/01 2005, doi: 10.1590/S1678-97412005000400012.

[5] H. Iwahashi, K. Yuri, and Y. Nosé, "Development of the oxygenator: Past, present, and future," *J. Artif. Organs,* Review vol. 7, no. 3, pp. 111-120, 2004, doi: 10.1007/s10047-004-0268-6.

[6] A. Mollahosseini, A. Abdelrasoul, and A. Shoker, "A critical review of recent advances in hemodialysis membranes hemocompatibility and guidelines for future development," *Materials Chemistry and Physics,* vol. 248, p. 122911, 2020/07/01/ 2020, doi: 10.1016/j.matchemphys.2020.122911.

[7] H. Wandt, K. Schäfer-Eckart, and A. Greinacher, "Platelet transfusion inhematology, oncology and surgery," *Deutsches Ärzteblatt International,* vol. 111, no. 48, pp. 809-815, 2014, doi: 10.3238/arztebl.2014.0809.

[8] TheEmergingRiskFactorsCollaboration, "Diabetes mellitus, fasting blood glucose concentration, and risk of vascular disease: a collaborative meta-analysis of 102 prospective studies," *The Lancet,* vol. 375, no. 9733, pp. 2215-2222, 2010/06/26/ 2010, doi: 10.1016/S0140-6736(10)60484-9.

[9] C. H. Heldin, B. Westermark, and A. Wasteson, "Platelet-derived growth factor. Isolation by a large-scale procedure and analysis of subunit composition," *The Biochemical journal,* Article vol. 193, no. 3, pp. 907-913, 1981, doi: 10.1042/bj1930907.

[10] O. Coskun, "Separation techniques: Chromatography," (in eng), *North Clin Istanb,* vol. 3, no. 2, pp. 156-160, 2016, doi: 10.14744/nci.2016.32757.

[11] A. Mollahosseini, A. Abdelrasoul, and A. Shoker, "Latest advances in zwitterionic structures modified dialysis membranes," *Materials Today Chemistry,* vol. 15, p. 100227, 2020/03/01/ 2020, doi: 10.1016/j.mtchem.2019.100227.

[12] P. Aimar *et al.*, "MOSAIC 3D Project Proposal," ed, 2017.

[13] S. W. Kim, "Platelet-Protein Interactions: Role of Proteins in Platelet Aggregation and Adhesion," in *Artificial Organs: Proceedings of a seminar on the clinical applications of membrane oxygenators and sorbent-based systems in kidney and liver failure and drug overdose, held at the University of Strathclyde, Glasgow, in August,*

1976, R. M. Kenedi, J. M. Courtney, J. D. S. Gaylor, T. Gilchrist, and S. M. Gerard Eds. London: Macmillan Education UK, 1977, pp. 273-279.

[14] Z. M. Ruggeri and S. P. Jackson, "Chapter 20 - Platelet Thrombus Formation in Flowing Blood," in *Platelets (Third Edition)*, A. D. Michelson Ed.: Academic Press, 2013, pp. 399-423.

[15] B. Savage, E. Saldívar, and Z. M. Ruggeri, "Initiation of platelet adhesion by arrest onto fibrinogen or translocation on von Willebrand factor," *CELL,* Article vol. 84, no. 2, pp. 289-297, 1996, doi: 10.1016/S0092-8674(00)80983-6.

[16] M. A. Packham, G. Evans, M. F. Glynn, and J. F. Mustard, "The effect of plasma proteins on the interaction of platelets with glass surfaces," *J. Lab. Clin. Med.,* Article vol. 73, no. 4, pp. 686-697, 1969.

[17] S. Chen, L. Li, C. Zhao, and J. Zheng, "Surface hydration: Principles and applications toward low-fouling/nonfouling biomaterials," *Polymer,* vol. 51, no. 23, pp. 5283-5293, 2010/10/29/ 2010, doi: 10.1016/j.polymer.2010.08.022.

[18] Y. C. Chiag, Y. Chang, W. Y. Chen, and R. C. Ruaan, "Biofouling resistance of ultrafiltration membranes controlled by surface self-assembled coating with PEGylated copolymers," *Langmuir,* Article vol. 28, no. 2, pp. 1399-1407, 2012, doi: 10.1021/la204012n.

[19] A. Venault, J.-R. Wu, Y. Chang, and P. Aimar, "Fabricating hemocompatible bi-continuous PEGylated PVDF membranes via vapor-induced phase inversion," *Journal of Membrane Science,* vol. 470, pp. 18-29, 2014/11/15/ 2014, doi: 10.1016/j.memsci.2014.07.014.

[20] A. Venault, M. R. B. Ballad, Y.-H. Liu, P. Aimar, and Y. Chang, "Hemocompatibility of PVDF/PS-b-PEGMA membranes prepared by LIPS process," *Journal of Membrane Science,* vol. 477, pp. 101-114, 2015/03/01/ 2015, doi: 10.1016/j.memsci.2014.12.024.

[21] H. G. Schild, "Poly(N-isopropylacrylamide): experiment, theory and application," *Progress in Polymer Science,* vol. 17, no. 2, pp. 163-249, 1992/01/01/ 1992, doi: 10.1016/0079-6700(92)90023-R.

[22] Y. Chang *et al.*, "Tunable bioadhesive copolymer hydrogels of thermoresponsive poly(N -isopropyl acrylamide) containing zwitterionic polysulfobetaine," *Biomacromolecules,* Article vol. 11, no. 4, pp. 1101-1110, 2010, doi: 10.1021/bm100093g.

[23] A. Venault *et al.*, "Stimuli-responsive and hemocompatible pseudozwitterionic interfaces," *Langmuir,* Article vol. 31, no. 9, pp. 2861-2869, 2015, doi: 10.1021/la505000m.

[24] G. Zhao and W. N. Chen, "Design of poly(vinylidene fluoride)-g-p(hydroxyethyl methacrylate-co-N-isopropylacrylamide) membrane via surface modification for enhanced fouling resistance and release property," *Appl Surf Sci,* Article vol. 398, pp. 103-115, 2017, doi: 10.1016/j.apsusc.2016.11.138.

[25] N. G. Patel, J. P. Cavicchia, G. Zhang, and B.-m. Zhang Newby, "Rapid cell sheet detachment using spin-coated pNIPAAm films retained on surfaces by an

aminopropyltriethoxysilane network," *Acta Biomaterialia,* vol. 8, no. 7, pp. 2559-2567, 2012/07/01/ 2012, doi: 10.1016/j.actbio.2012.03.031.

[26] S. Yu *et al.*, "Interaction of human serum albumin with short polyelectrolytes: A study by calorimetry and computer simulations," *Soft Matter,* Article vol. 11, no. 23, pp. 4630-4639, 2015, doi: 10.1039/c5sm00687b.

[27] S. Takeoka, Y. Teramura, Y. Okamura, M. Handa, Y. Ikeda, and E. Tsuchida, "Fibrinogen-conjugated albumin polymers and their interaction with platelets under flow conditions," *Biomacromolecules,* Article vol. 2, no. 4, pp. 1192-1197, 2001, doi: 10.1021/bm015554o.

[28] I. C. Peng *et al.*, "Continuous harvest of stem cells via partial detachment from thermoresponsive nanobrush surfaces," *Biomaterials,* vol. 76, pp. 76-86, 2016/01/01/ 2016, doi: 10.1016/j.biomaterials.2015.10.039.

[29] M. Kallioinen and M. Nyström, "Membrane Surface Characterization," in *Advanced Membrane Technology and Applications*: John Wiley & Sons, Inc., 2008, pp. 841-877.

[30] D. J. Johnson, D. L. Oatley-Radcliffe, and N. Hilal, "State of the art review on membrane surface characterisation: Visualisation, verification and quantification of membrane properties," *Desalination,* Review vol. 434, pp. 12-36, 2018, doi: 10.1016/j.desal.2017.03.023.

[31] H. Chang, T. Li, B. Liu, C. Chen, Q. He, and J. C. Crittenden, "Smart ultrafiltration membrane fouling control as desalination pretreatment of shale gas fracturing wastewater: The effects of backwash water," *Environment International,* vol. 130, p. 104869, 2019/09/01/ 2019, doi: 10.1016/j.envint.2019.05.063.

[32] O. Thygesen, M. A. B. Hedegaard, A. Zarebska, C. Beleites, and C. Krafft, "Membrane fouling from ammonia recovery analyzed by ATR-FTIR imaging," *Vibrational Spectroscopy,* Article vol. 72, pp. 119-123, 2014, doi: 10.1016/j.vibspec.2014.03.004.

[33] L. Benavente *et al.*, "FTIR mapping as a simple and powerful approach to study membrane coating and fouling," *Journal of Membrane Science,* Article vol. 520, pp. 477-489, 2016, doi: 10.1016/j.memsci.2016.07.061.

[34] "Product Specification." Sigma-Aldrich. https://www.sigmaaldrich.com/Graphics/COfAInfo/SigmaSAPQM/SPEC/74/747009/747009-BULK_____ALDRICH__.pdf (accessed March 9, 2020).

[35] A. Volkov, "Membrane Compaction," in *Encyclopedia of Membranes*, E. Drioli and L. Giorno Eds. Berlin, Heidelberg: Springer Berlin Heidelberg, 2015, pp. 1-2.

[36] B. C. Smith, *Fundamentals of Fourier Transform Infrared Spectroscopy*, 2nd ed. Boca Raton, FL: CRC Press, 2011, pp. 1-183.

[37] G. Socrates, *Infrared and Raman Characteristic Group Frequencies: Tables and Charts*, 3rd ed. Chichester: John Wiley & Sons, LTD, 2001.

[38] M. Todica, R. Stefan, C. V. Pop, and L. Olar, "IR and Raman investigation of some poly(acrylic) acid gels in aqueous and neutralized state," *Acta Phys Pol A,* Article vol. 128, no. 1, pp. 128-135, 2015, doi: 10.12693/APhysPolA.128.128.

[39] N. J. Lin *et al.*, "Surface self-assembled pegylation of fluoro-based pvdf membranes via hydrophobic-driven copolymer anchoring for ultra-stable biofouling resistance," *Langmuir,* Article vol. 29, no. 32, pp. 10183-10193, 2013, doi: 10.1021/la401336y.

[40] P. Bacchin, Y. Chang, A. Venault, and P. Aimar, "Modeling the resistance to fouling of PEGylated membranes," Unpublished paper.

[41] S. Alexander, "ADSORPTION OF CHAIN MOLECULES WITH A POLAR HEAD. A SCALING DESCRIPTION," *J Phys (Paris),* Article vol. 38, no. 8, pp. 983-987, 1977, doi: 10.1051/jphys:01977003808098300.

[42] I. Szleifer, "Protein Adsorption on Surfaces with Grafted Polymers: A Theoretical Approach," *Biophysical Journal,* vol. 72, no. 2, Part 1, pp. 595-612, 1997/02/01/ 1997, doi: 10.1016/S0006-3495(97)78698-3.

[43] A. Venault, Y. Chang, H. S. Yang, P. Y. Lin, Y. J. Shih, and A. Higuchi, "Surface self-assembled zwitterionization of poly(vinylidene fluoride) microfiltration membranes via hydrophobic-driven coating for improved blood compatibility," *Journal of Membrane Science,* Article vol. 454, pp. 253-263, 2014, doi: 10.1016/j.memsci.2013.11.050.

[44] A. Venault *et al.*, "A combined polymerization and self-assembling process for the fouling mitigation of PVDF membranes," *Journal of Membrane Science,* Article vol. 547, pp. 134-145, 2018, doi: 10.1016/j.memsci.2017.10.040.

[45] C. C. Yeh *et al.*, "Universal Bioinert Control of Polystyrene Interfaces via Hydrophobic-Driven Self-Assembled Surface PEGylation with a Well-Defined Block Sequence," *Macromol. Chem. Phys.,* Article vol. 218, no. 19, 2017, Art no. 1700102, doi: 10.1002/macp.201700102.

[46] S. H. Tang, A. Venault, C. Hsieh, G. V. Dizon, C. T. Lo, and Y. Chang, "A bio-inert and thermostable zwitterionic copolymer for the surface modification of PVDF membranes," *Journal of Membrane Science,* Article vol. 598, 2020, Art no. 117655, doi: 10.1016/j.memsci.2019.117655.

[47] F. Senusi, M. Shahadat, and S. Ismail, "Treatment of emulsion oil using tannic acid/tetraethylenepentamine-supported polymeric membrane," *Int. J. Environ. Sci. Technol.,* Article vol. 16, no. 12, pp. 8255-8266, 2019, doi: 10.1007/s13762-019-02233-6.

[48] C. A. D. Caro and C. Haller, *UV/VIS Spectrophotometry - Fundamentals and Applications*. Mettler Toledo, 2015, p. 53.

[49] L.-F. Fang *et al.*, "Improved antifouling properties of polyvinyl chloride blend membranes by novel phosphate based-zwitterionic polymer additive," *Journal of Membrane Science,* vol. 528, pp. 326-335, 2017/04/15/ 2017, doi: 10.1016/j.memsci.2017.01.044.

[50] F. Li, R. M. Guijt, and M. C. Breadmore, "Nanoporous Membranes for Microfluidic Concentration Prior to Electrophoretic Separation of Proteins in Urine," *Analytical Chemistry,* vol. 88, no. 16, pp. 8257-8263, 2016/08/16 2016, doi: 10.1021/acs.analchem.6b02096.

[51] L. Benavente, "Low fouling membranes for water and biotech applications " PhD thesis, Laboratoire de Génie Chimique de Toulouse, University of Toulouse 3 Paul Sabatier, Toulouse, 2016. [Online]. Available: http://thesesups.ups-tlse.fr/3336/

[52] D. Snisarenko, "Medium sized molecules clearance through artifical kidneys," PhD thesis, Laboratoire de Génie Chimique de Toulouse, University of Toulouse 3 Paul Sabatier, Toulouse, 2016. [Online]. Available: http://theses.fr/2016TOU30270/document

[53] W. Zhang, M. Wahlgren, and B. Sivik, "Membrane Characterization by the Contact Angle Technique: II. Characterization of UF-Membranes and Comparison between the Captive Bubble and Sessile Drop as Methods to obtain Water Contact Angles," *Desalination,* vol. 72, no. 3, pp. 263-273, 1989/12/01/ 1989, doi: 10.1016/0011-9164(89)80011-6.

[54] R. S. Hebbar, A. M. Isloor, and A. F. Ismail, "Chapter 12 - Contact Angle Measurements," in *Membrane Characterization*, N. Hilal, A. F. Ismail, T. Matsuura, and D. Oatley-Radcliffe Eds.: Elsevier, 2017, pp. 219-255.

[55] Y. Baek, J. Kang, P. Theato, and J. Yoon, "Measuring hydrophilicity of RO membranes by contact angles via sessile drop and captive bubble method: A comparative study," *Desalination,* vol. 303, pp. 23-28, 2012/10/01/ 2012, doi: 10.1016/j.desal.2012.07.006.

[56] M. J. Rosa and M. N. de Pinho, "Membrane surface characterisation by contact angle measurements using the immersed method," *Journal of Membrane Science,* vol. 131, no. 1, pp. 167-180, 1997/08/06/ 1997, doi: 10.1016/S0376-7388(97)00043-4.